Durability of cementitious materials in seawater environment: A review on chemical interactions, hardened-state properties and environmental factors

Matthew Zhi Yeon Ting and Yaolin Yi*

Matthew Zhi Yeon, Ting

School of Civil and Environmental Engineering, Nanyang Technological University, 639798, Singapore

Email: matthewzhiyeon.ting@ntu.edu.sg

Yaolin, Yi (*Corresponding author)

School of Civil and Environmental Engineering, Nanyang Technological University, 639798, Singapore

Email: yiyaolin@ntu.edu.sg

Abstract

Global warming-induced sea level rise exacerbates the deterioration of maritime structures and imperils their long-term durability. Cementitious materials such as ordinary Portland cement (OPC), pozzolanic blended cement (PBC) and alkali-activated material (AAM) can chemically interact with seawater, leading to degradation of binding properties. Despite their extensive applications in construction industry, the seawater resistance of these materials remains elusive. The objective of this work is to review and compare the durability of OPC, PBC and AAM in seawater environment from the perspectives of chemical interactions and hardened-state properties. This paper first briefly explains the mechanism of seawater intrusion into hardened cementitious materials. The chemical interactions of chloride, sulphate and carbon dioxide from seawater with hydrate components in OPC, PBC and AAM are discussed. From the durability aspects, this study evaluates and compares the performance of cementitious materials, including compressive strength, mass change, porosity and water absorption, and chloride permeability. Seawater deterioration mechanisms coupled with environmental factors such as wetting-drying cycle, external loading and temperature are also presented. Based on the review, future research is suggested to improve the durability studies related to seawater attack. This review provides better insight into the development of sustainable seawater-resistant construction materials for applications in seawater environment.

Keywords: Cementitious binder, deterioration, durability, seawater, wetting-drying cycle

1. Introduction

The rapidly growing construction industry over the last few decades has significantly increased greenhouse gas emissions, contributing to global warming and hence sea level rise [1, 2]. According to recent studies, global sea level is projected to rise by 0.25 m to 0.3 m by 2050 [3] and 0.6 m to 1.1 m by 2100 [4] if the emissions continue unabated. The sea level rise can consequently increase the exposure of maritime structures to seawater attack, accelerating material deterioration. Additionally, global warming can lead to extreme events such as coastal flooding [5], intensified wave activity [6] and increased tidal range [7]. Existing structures that have been designed using outdated guideline or without taking seawater attack into account may no longer meet the durability requirements and may experience premature deterioration. This will be a major concern for structures made of cementitious materials, which are vulnerable to seawater-induced durability issues, such as corrosion, sulphate attack, carbonation, hydrate leaching and strength deterioration [8]. Therefore, further research to evaluate the seawater resistance of cementitious materials is essential.

Cementitious materials can be divided into several types based on their hydration mechanisms. Ordinary Portland cement (OPC) is one of the most commonly used cementitious materials in construction and building works. The hydration of OPC involves the conversion of tri-calcium silicate (C_3S) into calcium silicate hydrate (C-S-H) and calcium hydroxide (CH) [9, 10]. C-S-H is the main binder that contributes to strength, whereas CH is a secondary hydration product that typically has low phase stability in aggressive environments. To improve binding properties, pozzolans, such as fly ash (FA) [11], silica fume (SF) [12], ground granulated blast furnace slag (GGBS) [13] and metakaolin (MK) [14], can be blended with OPC to form pozzolanic blended cement (PBC). The pozzolans contain silica (SiO_2) and alumina (Al_2O_3) in reactive crystalline form, which can react with CH to produce C-S-H and calcium aluminate silicate hydrate (C-A-S-H). Meanwhile, the binding properties of these alumina/silicate-rich

materials can also be activated by alkali solution, and this type of binder is known as alkali-activated material (AAM). During AAM hydration, polymerization and silicate condensation occur, which produces hydrates such as C-S-H, C-A-S-H and sodium aluminate silicate hydrate (N-A-S-H) [15, 16]. Due to the varying contents of hydration products from OPC, PBC and AAM, the deteriorating effects of seawater attack can differ. Thus, to better understand the deterioration mechanisms, it is crucial to evaluate and compare the interactions of seawater with OPC, PBC and AAM.

Seawater has properties that vary depending on geographical locations. The density of seawater is about 1.025 g/cm^3 at an ambient temperature of 25 ^{o}C [17]. Seawater is typically alkaline, with pH values ranging from 7.4 to 8.2, and these properties are attributed to the presence of salt [18]. Based on the published literature [19], the salinity of seawater in various marine regions could range from 0.6% to 4.8%, with a generally accepted average salinity of 3.5%. The chloride (Cl^-) and sulphate (SO_4^{2-}) contents of seawater account for 46.6%–77.5% and 4.9%–19.1% of total salt, respectively. In addition, increased carbon dioxide (CO_2) emissions can be absorbed and dissolved in seawater to form carbonic acid, contributing to ocean acidification [20]. The chemical interactions of these components in seawater with cementitious materials could reduce hydrate stability and cause hydrate leaching, compromising long-term material durability.

Previous research has studied and summarized the effect of seawater attack on cementitious materials performance. Mangi et al. [21] briefly reviewed the engineering properties of cementitious materials subjected to seawater attack, but the study was limited to assessing strength and chloride penetration, which was insufficient to explain the deterioration mechanism. A thorough study of the interactions of individual seawater components with cementitious binder is essential to comprehend the seawater attack mechanism. Recent studies [8, 19] have provided a more detailed review of the deterioration of OPC and PBC in marine

environment, but these studies have reached different conclusions. Qu et al. [8] showed that PBC was more durable than OPC, whereas Yi et al. [19] found that PBC was less stable in seawater environment due to its lower alkalinity. As a result, further investigation is still needed to iron out the discrepancy. Furthermore, the seawater resistance of AAM has not been reported in these studies. Although OPC, PBC and AAM are widely used in the construction industry, their seawater resistance has not been systematically documented and compared. Therefore, the aim of this study is to provide a critical review on the durability of OPC, PBC and AAM in seawater environment.

This review first delves into the mechanisms of seawater intrusion in hardened cementitious materials. The chemical interactions of seawater with cementitious materials are then reviewed. The impacts of seawater on the hardened-state properties are discussed. Lastly, the effects of environmental factors such as wetting-drying cycle, external loading and temperature on seawater attack are presented.

2. Seawater transport mechanisms in hardened cementitious materials

The cementitious materials can be exposed to seawater both internally (as mixing water) and externally (in service). The influence of seawater used as mixing water is not included in this study as it has been discussed elsewhere [18, 22, 23].

External seawater attack requires seawater infiltration into cementitious paste from the outside via porous structure. The contact between external aqueous media and pore solution alters fluid hydrostatic equilibrium, creating net mass flow. The seawater penetration and ionic transport caused by aqueous solution motion is dominated by saturated and unsaturated flows [24]. Figure 1 shows the mass flow in cementitious matrix generated by surface water hydraulic pressure (ϕ). The saturation degree (θ) maps out the zones of water flow, namely saturated zone

near the surface with pores totally filled with water, unsaturated zone with saturation degree of 0<θ<1, and dry zone with pores completely dry.

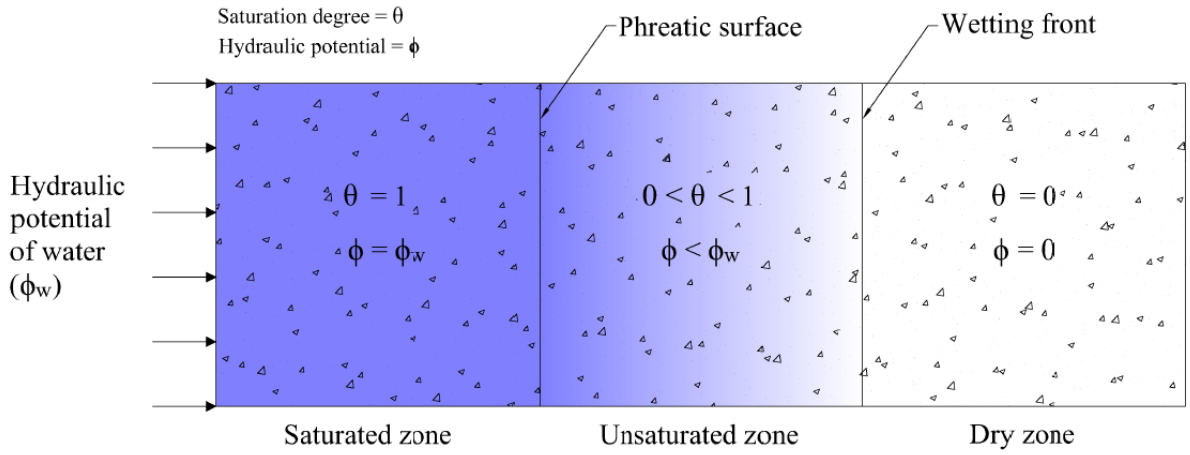

Figure 1. Water flow in porous cementitious matrix under hydraulic pressure [24, 25]

In unsaturated condition, absorption and permeation are the main transport mechanisms in cementitious materials [25]. Absorption is defined as water uptake through capillary suction induced by partially saturated state of pore structure. Permeation is the transport of water into cementitious matrix in response to hydraulic pressure gradient. Due to the low porosity of cementitious materials, water movement is restricted to low volume flow and is regarded as laminar flow. The extended Darcy's law, as shown in Equation (1), can be used to describe the unsaturated flow in cementitious materials [26].

$$q = -\frac{\rho}{\eta} K \cdot \theta \cdot \phi \quad (1)$$

where q is flow rate, ρ is water density, η is water viscosity, K is unsaturated permeability, θ is degree of saturation and ϕ is hydraulic potential of water.

In saturated condition with no hydraulic potential gradient, the velocity of liquid is considered null. The ionic transport of seawater is mainly driven by electrochemical potential gradient. Diffusion, induced by chemical potential difference, transfers solutes from high concentration region to low concentration region [27]. Electrical coupling or electrical potential gradient is

also formed as a result of varying velocity of charged ions, in which faster ions accelerate slower ions via mutual attraction caused by opposite ionic charges [28].

There are other transport processes can affect the ionic movement in pore solution under saturated condition. The chemical reactivity of ionic species, such as ion-ion and ion-solvent interactions, has effect on the ionic flux, particularly in solution with high ionic strength [29]. Thermal diffusion arising from gradient in non-isothermal condition facilitates ionic flux through the Soret effect [30]. The temperature difference also affects the ionic reactivity in pore solution by altering the solubility constant [31]. In brief, ionic transport in cementitious materials under saturated condition can be determined using the extended Nernst-Planck equation as shown in Equation (2) [28]. The R term in Equation (2) accounts for the change in local availability of ions in pore solution as a result of chemical interactions with cementitious materials, which is discussed in Section 3.

$$\frac{\partial(wc_i)}{\partial t} = \frac{\partial}{\partial x}\left(\underbrace{D_i w\frac{\partial c_i}{\partial x}}_{\text{diffusion}} + \underbrace{wc_i\frac{D_i z_i F}{rT}\frac{\partial \psi}{\partial x}}_{\text{electrical coupling}} + \underbrace{wD_i c_i\frac{\partial \ln\gamma_i}{\partial x}}_{\text{chemical reactivity}} + \underbrace{\frac{wD_i c_i \ln(\gamma_i c_i)}{T}w\frac{\partial T}{\partial x}}_{\text{temperature}}\right) - R \quad (2)$$

where w is volumetric water content, c_i is concentration of ion *i* in solution, D_i is diffusion coefficient, z_i is valence number of ion *i*, F is Faraday constant, r is ideal gas constant, T is temperature of solution, ψ is electrical potential and γ_i is chemical activity coefficient.

3. Chemical interactions of cementitious materials with seawater

To better understand the deterioration of cementitious materials, it is essential to examine their chemical interactions with seawater. This section discusses the chemical reactions of seawater with OPC, PBC and AAM.

3.1. *Ordinary Portland cement (OPC)*

3.1.1. *OPC with chloride*

Chloride is one of the main components in seawater that can react with OPC. Aluminate ferrite mono (AFm), tri-calcium aluminate (C_3A) and CH from OPC react with chloride to form Friedel's salt (FS) ($3CaO•Al_2O_3•CaCl_2•10H_2O$) as shown in Equation (3) [8]. The formation of FS involves two mechanisms, namely adsorption and anion-exchange [32]. FS is produced in the former mechanism when chloride adsorbs on $[Ca_2Al•(OH^-)_6•2H_2O]^+$ of AFm. The latter mechanism involves exchange of chloride with hydroxide (OH^-) of AFm. Moreover, Kuzel's salt (KS) ($3CaO•Al_2O_3•0.5CaCl_2•0.5CaSO_4•10H_2O$), a chloro-sulphoaluminate AFm phase, is another product of reaction between chloride and AFm, as depicted in Equation (4) [33, 34]. KS has crystal structure that is made up of intercalation of FS and AFm [35]. FS can partially convert to KS when exposed to low-chloride environment. The majority of studies [11, 36-38] reveal that FS and KS have no negative impact on OPC. FS promotes hydration of aluminate (C_3A) and ferrite (C_4AF), which could increase chloride binding capacity. The precipitation of FS also densifies pore structure and reduces permeability.

$$3CaO•Al_2O_3•6H_2O + Ca(OH)_2 + 2Cl^- + 4H_2O \rightarrow 3CaO•Al_2O_3•CaCl_2•10H_2O \text{ (Friedel's salt)} + 2OH^- \quad (3)$$

$$3CaO•Al_2O_3•6H_2O + 0.5Ca(OH)_2 + 0.5CaSO_4 + Cl^- + 4H_2O \rightarrow 3CaO•Al_2O_3•0.5CaCl_2•0.5CaSO_4•10H_2O \text{ (Kuzel's salt)} + OH^- \quad (4)$$

Another chloride reaction is the interaction of CH with calcium chloride ($CaCl_2$), which produces calcium oxychloride (CAOXY) [$3Ca(OH)_2•CaCl_2•12H_2O$] as illustrated in Equation (5) [39-41]. CAOXY exists in the atmosphere at temperature of 0–40^oC and has three times the volume of CH [42]. CAOXY crystals are prismatic and plate-shaped, and their precipitations are expansive, which can cause destructive stress on pore. The leaching of calcium from CH during CAOXY formation leads to hydrate dilution and hence binding strength loss. When

magnesium chloride ($MgCl_2$) is involved in the reaction, the damage is more severe due to the formation of brucite [$Mg(OH)_2$] and magnesium oxychloride [$Mg(OH)_2 \cdot MgCl_2 \cdot 8H_2O$] as shown in Equations (6) and (7) [43]. The damage is exacerbated by the dissolution of C-S-H and formation of magnesium silicate hydrate (M-S-H) that has weaker cementitious property.

$$CaCl_2 + 3Ca(OH)_2 + 12H_2O \rightarrow 3Ca(OH)_2 \cdot CaCl_2 \cdot 12H_2O \text{ (Calcium oxychloride)} \quad (5)$$

$$Ca(OH)_2 + MgCl_2 \rightarrow Mg(OH)_2 \text{ (Brucite)} + CaCl_2 \quad (6)$$

$$Mg(OH)_2 + MgCl_2 + 8H_2O \rightarrow Mg(OH)_2 \cdot MgCl_2 \cdot 8H_2O \text{ (Magnesium oxychloride)} \quad (7)$$

3.1.2. OPC with sulphate

Sulphate is another seawater component that can react with OPC. It is commonly found in seawater as sodium sulphate (Na_2SO_4) and magnesium sulphate ($MgSO_4$) [44]. The sulphate reacts with C_3A, CH and mono-sulphate hydrate (C_4ASH_{12}) to form ettringite ($C_3A \cdot 3CaSO_4 \cdot 32H_2O$) and gypsum ($CaSO_4$), as shown in Equations (8)–(10) [45]. Ettringite and gypsum are formed within the pores of cementitious matrix and can cause 1.3 to 2.8 times volume expansion, resulting in cracking [46].

$$C_3A + 3SO_4^{2-} + 3Ca(OH)_2 + 32H_2O \rightarrow C_3A \cdot 3CaSO_4 \cdot 32H_2O \text{ (Ettringite)} + 6OH^- \quad (8)$$

$$Ca(OH)_2 + SO_4^{2-} \rightarrow CaSO_4 \text{ (Gypsum)} + 2OH^- \quad (9)$$

$$3C_4ASH_{12} + 3SO_4^{2-} \rightarrow 2C_3A \cdot 3CaSO_4 \cdot 32H_2O \text{ (Ettringite)} + 2Al(OH)_3 \quad (10)$$

$MgSO_4$ causes more severe deterioration than Na_2SO_4 as cation-exchange of Ca in C-S-H and CH occurs to form M-S-H and brucite, which reduces the binding capability, as shown in Equations (11) and (12) [47]. Hydrates decalcification increases porosity and degrades

mechanical properties. The production of brucite lowers the pH of pore solution and reduces the ability to bind chloride [48].

$$C\text{-}S\text{-}H + Mg^{2+} \rightarrow M\text{-}S\text{-}H + Ca^{2+} \quad (11)$$

$$Ca(OH)_2 + Mg^{2+} \rightarrow Mg(OH)_2 + Ca^{2+} \quad (12)$$

Besides, the coexistence of sulphate and chloride in seawater can influence the reactions with OPC. When exposed to NaCl solution, Yoon et al. [49] found lower amounts of ettringite formation during sulphate attack. The presence of chloride in seawater and its binding with AFm phase to form FS slow down the precipitation of ettringite. The FS also lowers CH concentration in pore solution, which converts ettringite into non-expansive and soluble low-basic compound [50]. On the other hand, sulphate can also diminish the amounts of FS in chloride reactions [51, 52]. Although the formation of FS is favored, FS can partially transform into ettringite, especially under high sulphate concentration. The chloride binding capability decreases because a fraction of AFm can interact with sulphate to form ettringite.

3.1.3. OPC with carbon dioxide

Carbon dioxide (CO_2) from the atmosphere can dissolve in seawater to react with CH and C-S-H to form calcium carbonate ($CaCO_3$) as illustrated in Equations (13) and (14) [53]. The reactions reduce the hydroxide concentration and lower the alkalinity in pore solution, affecting hydrate stability and inducing hydrate dissolution [54]. The development of calcite and depletion of C-S-H reduce the strength of OPC.

$$Ca(OH)_2 + CO_2 + H_2O \rightarrow CaCO_3 + 2H_2O \quad (13)$$

$$C\text{-}S\text{-}H + 2CO_2 \rightarrow 2CaCO_3 + SiO_2 + H_2O \quad (14)$$

Carbonation can influence the chloride reactions in OPC. The carbonation lowers the pH of pore solution and reduces the chloride binding capacity since FS and KS are decomposed into free chloride [55]. The carbonation also decreases the CH available for FS formation.

According to Chang et al. [56], the free chloride content in OPC paste could be increased by 50% after 56-day carbonation. The chloride convection zone was also expanded by threefold [57].

The presence of $CaCO_3$ induces another type of sulphate reactions with OPC. As shown in Equation (15), a combination of sulphate and carbonate can react with C-S-H to form thaumasite ($CaCO_3$•$CaSO_4$•$CaSiO_3$•$15H_2O$), a non-cementitious compound [46]. The transformation of C-S-H into thaumasite weakens the binding strength of OPC. Sibbick et al. [58] showed that mortar sampled from the harbor walls after three years of suphate attack was porous and poorly degraded, with cement paste containing thaumasite in considerable amounts. The reaction in Equation (15) is more favored at low temperatures ranging from 0 to 15^{o}C, because this temperature range facilitates the transition-state intermediate for thaumasite precipitation [46, 59].

$$CaCO_3 + CaSO_4 + \text{C-S-H} + H_2O \rightarrow \underset{\text{(Thaumasite)}}{CaCO_3 \bullet CaSO_4 \bullet CaSiO_3 \bullet 15H_2O} \quad (15)$$

3.2. Pozzolanic blended cement (PBC)

3.2.1. PBC with chloride

Pozzolans are supplementary cementitious materials that can partially replace OPC to enhance binding properties. Pozzolanic reaction in PBC refers to the chemical reaction of silica and alumina with CH to form C-S-H and C-A-S-H. Since the main reactant CH, as shown in Equations (3)–(6), is consumed in pozzolanic reaction, the reactivity of PBC with chloride decreases. Past studies [39, 40] show that incorporation of reactive pozzolans like Class-F FA and GGBS can impede the formation of CAOXY. The alumina in PBC is also capable of binding chloride in the form of FS and KS [60]. The increased C-S-H content in PBC densifies pore structure and reduces chloride permeability. Some studies [39, 61] show that the hydration of alumina in PBC produces C-S-H with low calcium-to-silicon (Ca/Si) ratio and hence low

chloride binding capability. However, it has little effect on the overall chloride binding capacity since the alumina hydration is secondary in PBC.

3.2.2. PBC with sulphate

The sulphate attack resistance of PBC was generally higher than the OPC due to the following factors. First, the pozzolanic reaction produces more C-S-H that boosts the strength of PBC. Second, the CH content in PBC is low, leading to a less localized ettringite precipitation [44, 59]. Third, the partial replacement of OPC with pozzolans lowers the overall C_3A content, which limits the development of ettringite and gypsum.

Although PBC contains considerable amounts of alumina, its reaction with CH is advantageous in preventing sulphate attack. During pozzolanic reaction, CH binds with alumina to produce hydrotalcite [62, 63]. Since the alumina bound in hydrotalcite is inert, it will not contribute to the production of ettringite. However, pozzolans with low reactivity can result in more alumina available for ettringite formation. Ogawa et al. [64] revealed that, while the hydration of GGBS reduced the sulphate ingress, unreacted alumina might still transform into ettringite. Hence, an optimum replacement ratio and proper curing methods are essential to achieve the benefits of PBC in terms sulphate resistance.

Some studies [44, 48] show that PBC is more susceptible to $MgSO_4$ attack than OPC. Aye and Oguchi [48] found that the strength loss of SF mortar and FA mortar in $MgSO_4$ attack was 9% and 2% more than that of OPC mortar. Nehdi and Hayek [44] reported that PBC mortar exposed to $MgSO_4$ solution was significantly damaged with surface scaling and mass loss, whereas the OPC mortar exhibited less surface deterioration. The pozzolanic reaction of PBC consumes CH and reduces the pH buffer in pore solution, resulting in cation exchange between $MgSO_4$ and C-S-H. The $MgSO_4$ attack causes decalcification, in which the Mg^{2+} cations react with C-S-H and form cohesionless M-S-H.

3.2.3. PBC with carbon dioxide

The CO_2 reactions deteriorate PBC more severely than OPC. As CH is consumed during pozzolanic reaction, the cementitious matrix loses pH buffer, resulting in direct carbonation of C-S-H. Besides, because the carbonation process occurs from the outer to the inner layer, the formation of $CaCO_3$ can generally act as a barrier to prevent further CO_2 penetration. However, since the concentration of $CaCO_3$ in PBC is low due to the reduced CH, the barrier becomes thinner, making the C-S-H more susceptible to carbonation. Moreover, the C-S-H formed in PBC has low Ca/Si ratio, which accelerates the carbonation process [65]. Other hydrates such as C-A-S-H and aluminate phase are amorphous and disordered, and can be easily degraded during carbonation [66].

3.3. Alkali-activated materials (AAM)

3.3.1. AAM with chloride

AAM binds chloride through surface adsorption on C-A-S-H and N-A-S-H gels [67]. The electrostatic charge between gels and chloride creates Van der Waals force for physical adsorption. Besides, the pore solution of AAM is alkaline, which exhibits high ionic strength and facilitates surface adsorption [68]. The hydrotalcite in AAM also contributes to chloride binding. The chloride pairing with sodium ions can be adsorbed on the diffuse layer of hydrotalcite [69]. Chloride is also bound by hydrotalcite when aluminate phases (C_3A) react with chloride via anion-exchange [70]. In addition, statlingite, is another AFm hydrate found in AAM that can bind chloride [71]. Chloride can be bound by statlingite through surface adsorption and lattice substitution.

3.3.2. AAM with sulphate

N-A-S-H and hydrotalcite in AAM are less reactive with sulphate and have high resistance to de-alumination [72-74]. However, sulphate can be physically adsorbed and bound on C-A-S-H through electrostatic force. This may promote the reactions between C-A-S-H and sulphate

to form ettringite and gypsum. Sulphate reactions with unreacted magnesia and aluminate in slag-based AAM can also form these deterioration products. Several published literatures [72, 73, 75] indicate that AAM is vulnerable to $MgSO_4$-induced sulphate attack. The Mg ions from $MgSO_4$ can replace the Ca ions in C-A-S-H and Na ions in N-A-S-H to form magnesium alumina-silicate hydrate (M-A-S-H). Expansive products of brucite and gypsum are also formed. Since AAM lacks buffering due to the absence of CH, its pH can drop rapidly during $MgSO_4$ attack, which results in decalcification of C-A-S-H [72, 75]. This decreases the molar ratio of Ca/Si, leading to further release of Ca ions from C-A-S-H. Nonetheless, the molar ratio of Al/Si in AAM will remain constant because de-alumination is less likely to occur.

3.3.3. AAM with carbon dioxide

When CO_2 interacts with C-A-S-H and N-A-S-H in AAM, carbonate compounds such as calcite, aragonite, vaterite, natron ($Na_2CO_3 \cdot 10H_2O$) and trona ($Na_2CO_3 \cdot NaHCO_3 \cdot 2H_2O$) are formed [76-78]. The carbonated C-A-S-H typically has a low Ca/Si ratio but contains a highly cross-linked alumina-silicate phase. The alumina-silicate phase is generally stable due to its highly polymerized structure. N-A-S-H, on the other hand, is more porous than C-A-S-H and thus more easily carbonated. The formation of natron and trona, also known as sodium carbonate and sodium bicarbonate, is responsible for the carbonation of N-A-S-H. N-A-S-H carbonation can occur in two stages: (i) carbonation of sodium hydrate to form sodium carbonate and (ii) establishment of phase equilibrium between carbonate and bicarbonate [79]. According to Zhang et al. [80], a high-alkalinity environment encourages carbonate formation, whereas a low-alkalinity environment favors bicarbonate formation. Nevertheless, the hydrotalcite phase in AAM is capable of decreasing the carbonation by acting as CO_2 sorbent [81].

3.4. Summary

OPC, PBC and AAM are susceptible to seawater attack due to interactions with chloride, sulphate and CO_2. Table 1 provides a summary of these chemical reactions. Chloride reactions cause minimal damage to the cementitious materials, as chloride can be effectively bound by hydration products such as FS, KS and hydrotalcite. On the other hand, sulphate reactions cause more severe damage due to the formation of deterioration products like ettringite, gypsum and brucite. The carbonation also depletes C-S-H and CH, reducing the binding properties of cementitious materials. Although the effects of chloride, sulphate and CO_2 have been evaluated individually, the literature review indicates that there exists a synergy among these components in the actual seawater environment. Thaumasite, for example, is formed through a combination of sulphate and carbonate reactions. The coexistence of chloride and sulphate also influences reactions of each other, affecting formation of FS and ettringite. However, there is still a lack of understanding on the mutual interactions of these seawater components. Furthermore, seawater compositions are not constant and vary in salinity, making it difficult to accurately assess seawater attack mechanisms. In this context, future study should look into the combined interactions of chloride, sulphate and CO_2 with cementitious materials in seawater by considering a wide range of composition ratios.

Table 1. Summary of seawater reactions with OPC, PBC and AAM

Cementitious materials	Reactants		Product	Findings	Ref
	In seawater	In binder			
OPC	1. Chloride				
	• Chloride ion (Cl^-)	• Tri-calcium aluminate ($3CaO•Al_2O_3•6H_2O$) • Calcium hydroxide ($Ca(OH)_2$)	• Friedel's salt ($3CaO•Al_2O_3•CaCl_2•10H_2O$)	• Forming through anion-exchange and adsorption on AFm • Immobilize chloride and densify pore structure, reducing permeability	[8, 32]
	• Chloride ion (Cl^-)	• Tri-calcium aluminate ($3CaO•Al_2O_3•6H_2O$) • Calcium hydroxide ($Ca(OH)_2$) • Calcium sulphate ($CaSO_4$)	• Kuzel's salt ($3CaO•Al_2O_3•0.5CaCl_2•0.5CaSO_4•10H_2O$)	• Similar properties to Friedel's salt, but exhibit lower chloride binding capability	[33, 34]
	• Calcium chloride ($CaCl_2$)	• Calcium hydroxide ($Ca(OH)_2$)	• Calcium oxychloride ($3Ca(OH)_2•CaCl_2•12H_2O$)	• Prismatic and plate-shaped crystals that are expansive • Reactions cause loss of hydrate	[39-41]
	• Magnesium chloride ($MgCl_2$)	• Calcium hydroxide ($Ca(OH)_2$) • Calcium silicate hydrate (C-S-H)	• Magnesium oxychloride ($Mg(OH)_2•MgCl_2•8H_2O$) • Magnesium silicate hydrate (M-S-H) • Brucite ($Mg(OH)_2$)	• More severe deterioration than CAOXY formation • Dissolution of C-S-H and hence strength loss	[43]
	2. Sulphate				
	• Sulphate ion (SO_4^{2-})	• Tri-calcium aluminate (C_3A) • Calcium hydroxide ($Ca(OH)_2$)	• Ettringite ($C_3A•3CaSO_4•32H_2O$) • Gypsum ($CaSO_4$)	• Form within pore to cause expansion and damage • Deplete hydrate, resulting in porous structure	[45]
	• Magnesium sulphate ($MgSO_4$)	• Calcium silicate hydrate (C-S-H) • Calcium hydroxide ($Ca(OH)_2$)	• Magnesium silicate hydrate (M-S-H) • Brucite ($Mg(OH)_4$)	• Cation exchange with C-S-H gel to form weaker M-S-H gel • Reduce pH and chloride binding	[47, 48]
	3. Carbon dioxide				
	• Carbon dioxide (CO_2)	• Calcium silicate hydrate (C-S-H) • Calcium hydroxide ($Ca(OH)_2$)	• Calcium carbonate ($CaCO_3$)	• Reduce pH and corrosion resistance • Decompose FS into free chloride • Dissolution C-S-H and reduce strength	[53, 54]

	• Calcium carbonate ($CaCO_3$) • Calcium sulphate ($CaSO_4$)	• Calcium silicate hydrate (C-S-H)	• Thaumasite ($CaCO_3$•$CaSO_4$•$CaSiO_3$•$15H_2O$)	• Non-cementitious compound formed at temperature of 0–15 °C • Reduce strength and cause cracking of cementitious materials	[46, 58, 59]
PBC	<u>1. Chloride</u>				
	• Chloride ion (Cl^-)	• Alumina (Al_2O_3)	• Friedel's salt ($3CaO$•Al_2O_3•$CaCl_2$•$10H_2O$)	• Immobilize free chloride • Bind less chloride due to low C-S-H with low Ca/Si ratio	[60, 61]
	<u>2. Sulphate</u>				
	• Magnesium sulphate ($MgSO_4$)	• Calcium silicate hydrate (C-S-H)	• Magnesium silicate hydrate (M-S-H)	• More severe damage than in OPC due to low CH content, resulting in direct reactions with C-S-H	[44, 48]
	<u>3. Carbon dioxide</u>				
	• Carbon dioxide (CO_2)	• Calcium silicate hydrate (C-S-H) • Calcium aluminate silicate hydrate (C-A-S-H) • Aluminate phase	• Calcium carbonate ($CaCO_3$)	• Low CH content accelerates carbonation of C-S-H • C-S-H with low Ca/Si ratio is more vulnerable to carbonation	[55, 65, 66]
AAM	<u>1. Chloride</u>				
	• Chloride ion (Cl^-)	• Aluminate phase (C_3A)	• Hydrotalcite • Statlingite	• Bind chloride through adsorption on hydrates surface	[67, 69, 71]
	<u>2. Sulphate</u>				
	• Magnesium sulphate ($MgSO_4$)	• Calcium aluminate silicate hydrate (C-A-S-H) • Sodium aluminate silicate hydrate (N-A-S-H)	• Magnesium aluminate silicate hydrate (M-A-S-H) • Brucite ($Mg(OH)_2$) • Gypsum ($CaSO_4$)	• High resistance to de-alumination during sulphate attack • Lack of CH increases vulnerability to cation exchange caused by $MgSO_4$	[72, 73, 75]
	<u>3. Carbon dioxide</u>				
	• Carbon dioxide (CO_2)	• Calcium aluminate silicate hydrate (C-A-S-H) • Sodium aluminate silicate hydrate (N-A-S-H)	• Calcite ($CaCO_3$) • Aragonite ($CaCO_3$) • Vaterite ($CaCO_3$) • Natron (Na_2CO_3•$10H_2O$) • Trona (Na_2CO_3•$NaHCO_3$•$2H_2O$)	• Carbonated C-A-S-H remains stable due to highly polymerized structure • N-A-S-H is more easily carbonated due to porous structure, forming carbonate and bicarbonate compounds	[76-78]

311

4. Hardened-state properties of cementitious materials exposed to seawater attack

The interactions of cementitious materials with seawater modify the hydrate phases and gel structures, as well as generates deterioration products, all of which have direct and considerable impacts on the durability properties. To elucidate the implications on durability, the hardened-state properties of cementitious materials after external seawater attack are discussed in this section.

4.1. Compressive strength variation

Compressive strength has been used in numerous investigations to measure the resistance of cementitious materials against seawater attack. In this study, the compressive strength variation caused by seawater attack is determined using data gathered from the literature. This analysis incorporates the experimental results for cementitious materials used in paste, mortar and concrete. Although the literature contains a variety of mixture proportions, the same cementitious mixture types have been used in the individual calculation for comparison.

Figure 2 to Figure 4 depict the compressive strength variation for OPC, PBC and AAM. The literature reveals inconsistent effects of seawater on the compressive strength, with some studies [14, 82-96] showing a decrease in strength and others [97-107] showing an increase in strength. The results disparity is attributed to two factors: curing age and exposure period. The literature in Figure 2 to Figure 4 has been grouped based on curing age of cementitious materials before seawater attack. Specimens with shorter curing times, such as 1, 5 and 7 days, generally experience strength gain due to the ongoing hydration. In this case, the hydration effect overwhelms the deterioration caused by seawater reactions. The seawater exposure period for each study is also shown in Figure 2 to Figure 4. The seawater attack is long-term process that causes more evident strength deterioration only after prolonged exposure periods (i.e. more than 365 days).

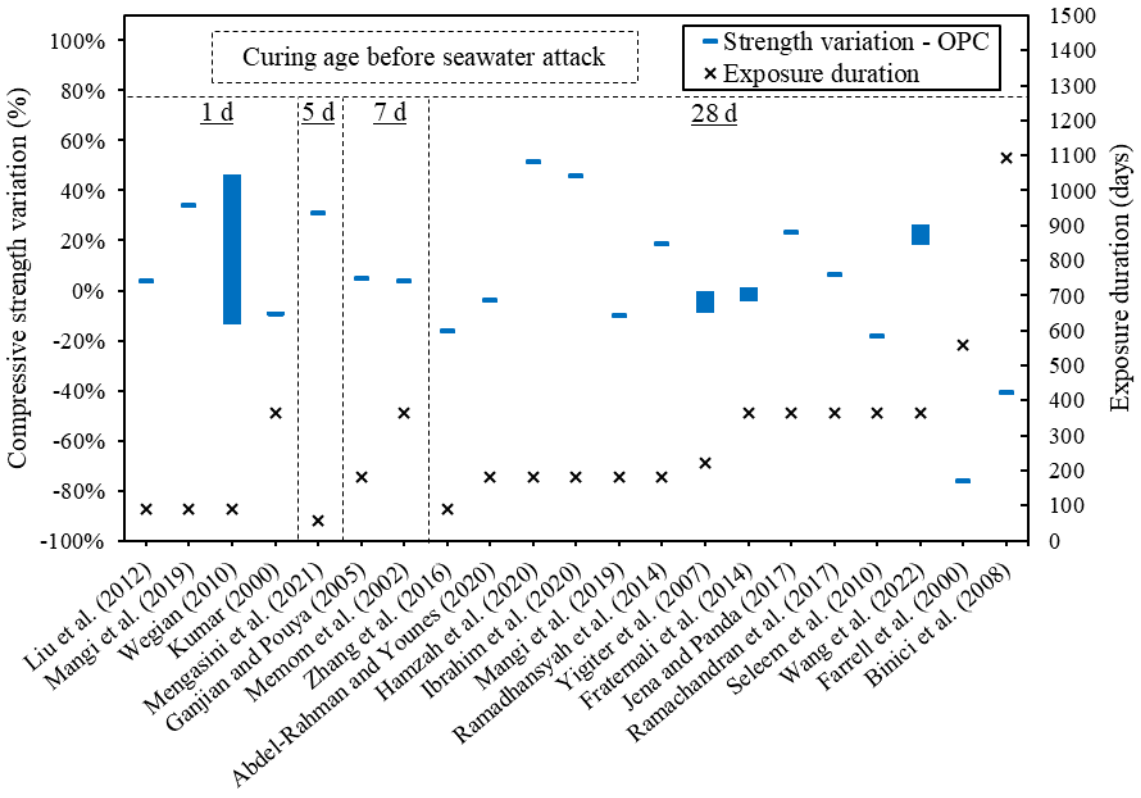

336

337 **Figure 2. Compressive strength variation of OPC under seawater attack (data adapted**

338 **from [82, 88-107])**

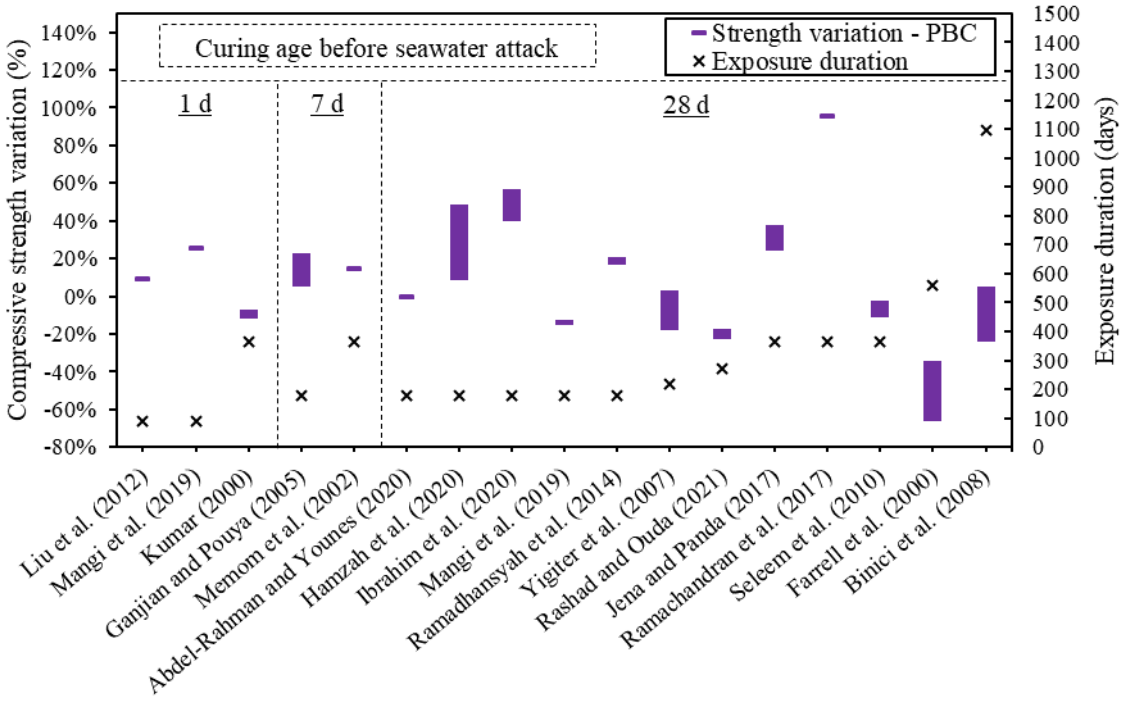

339

Figure 3. Compressive strength variation of PBC under seawater attack (data adapted from [14, 82, 90-93, 95-97, 99-105, 107])

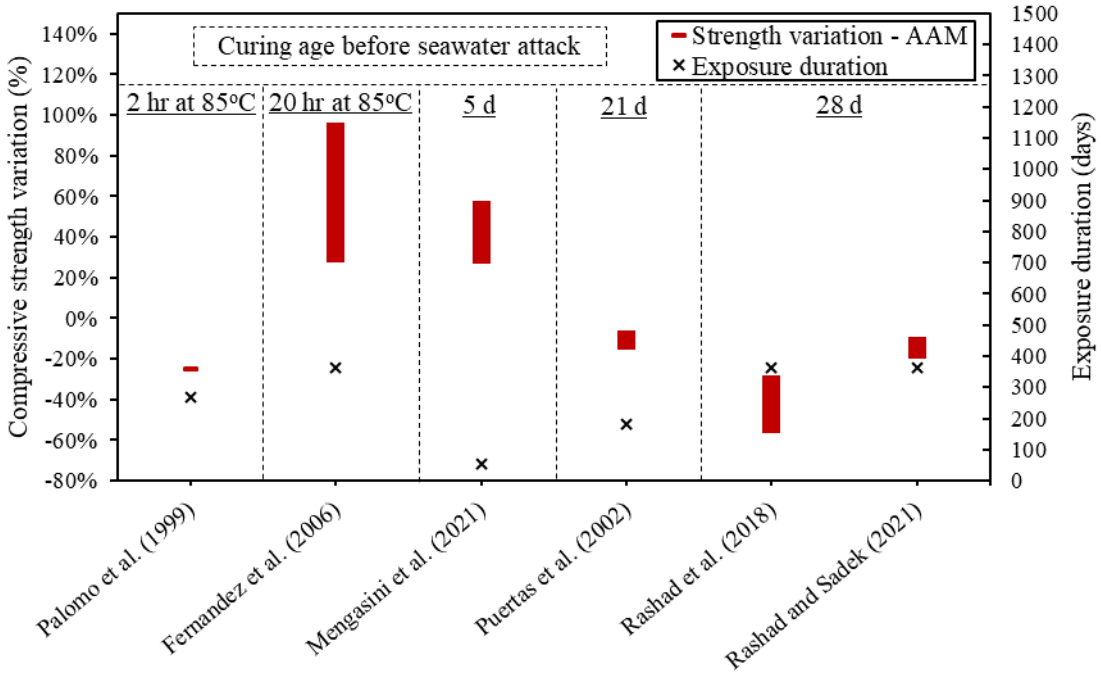

Figure 4. Compressive strength variation of AAM under seawater attack (data adapted from [83-87, 98])

There are several factors that contribute to the strength deterioration of cementitious materials. First, the chloride, sulphate and CO_2 from seawater gradually reacts with cementitious paste and decalcifies the C-S-H. Salt crystals also form on the surface of cement paste, causing crystallization pressure [95]. The seawater resistance of cementitious materials depends on the binder content. For example, increase in OPC content from 250 kg/m^3 to 350 kg/^{3} could reduce strength loss from 9% to nearly 0% [82]. Higher binder content increases paste volume and promotes better bonding. But, further increase in OPC content has detrimental effect due to higher C_3A content, which triggers sulphate attack [90]. Long-term seawater exposure causes significant strength loss. But, the strength loss will occur faster if seawater is high in salinity

and contains a huge quantity of sulphate salts, particularly $MgSO_4$, which can cause expansive damage and hydrate dissolution.

Some studies, however, show that seawater attack improves strength. The salt precipitated from seawater within the cementitious matrix can reduce porosity and enhance strength temporarily [103]. The cementitious matrix is also enhanced by filling of pores with Friedel's salt from chloride reactions. The formation of ettringite from sulphate reactions also densifies the pore structure. The cementitious matrix continues to hydrate during seawater attack, with the curing effect outweighs the seawater-induced damage. But, the curing effect diminishes as the exposure duration increases. Ibrahim et al. [105] showed that the strength gain of concrete peaked at 60 days, and decreased by 7%–13% at 180 days. Jaya et al. [97] reported that the peak strength gain occurred between 30 and 60 days. The delayed strength deterioration could be ascribed to the low salinity of seawater [106]. During this period, strength is gained due to pore densification, but it then declines due to over-accumulation of expansive products and loss of hydrate.

PBC and AAM are generally more resistant to seawater attack than OPC as shown in Figure 3 and Figure 4. OPC has the greatest compressive strength loss, with variation ranging from -76% to 51.4%. The use of PBC and AAM slightly reduces the strength loss, with variation of -50% to 95.2% and -42.1% to 62% respectively. The hydration of pozzolanic materials considerably enhances the strength, producing more hydrate gels to withstand expansive damage and resist hydrate dissolution. The conversion of CH into C-S-H compacts the pore structure and hence minimizes seawater intrusion. The use of ternary blended cements further lowers the strength degradation [103]. As for AAM, it has higher early strength than OPC, making it more resistant to seawater attack [98]. The use of thermal curing accelerates the hydration of AAM [86, 87]. Seawater promotes geo-polymerization of unreacted aluminate and silicate, which improves

strength and suppresses degradation [84]. AAM also contains fewer high-calcium phases and is less susceptible to seawater-induced decalcification.

In summary, the effect of seawater on compressive strength varies depending on curing conditions, curing methods, salinity and seawater compositions. The combination of seawater attack and ongoing hydration leads to inconsistent findings in the published literature. To improve the experimental study, another set of freshwater-exposed specimens should be included so that the strength variation caused by hydration in seawater and freshwater can be compared.

4.2. Mass change

Mass change is another property commonly used to assess the deterioration of cementitious materials. The mass can vary during seawater attack due to the generation of corrosive products and the dissolution of hydrate phases.

Figure 5 depicts the mass change of OPC, PBC and AAM during seawater attack. The exposure durations are normalized to the final test durations to better illustrate the mass variations. Several studies [93, 100, 102, 108] show that the mass change is two-stage process, with the first mass-increasing stage and the later mass-decreasing stage. Mangi et al. [100] found a mass increase of 0.9%–2.6% after 56 days, while the mass change fell to 0.3%–0.4% after 90 days. Liu et al. [102] showed that mass-increasing and mass-decreasing stages occurred at 0–60 days and 60–90 days respectively. Mangi et al. [93] reported that the highest mass gain was 2% and the mass-decreasing stage began after 30 days. The mass-increasing stage was caused by the formation of Friedel's salt, ettringite and gypsum within the pores. The hydration of cementitious materials also released more C-S-H that increased the mass. In the mass-decreasing stage, however, over-accumulation of these products caused expansion and cracking. The mass loss was also ascribed to the leaching of C-S-H and AFm phases.

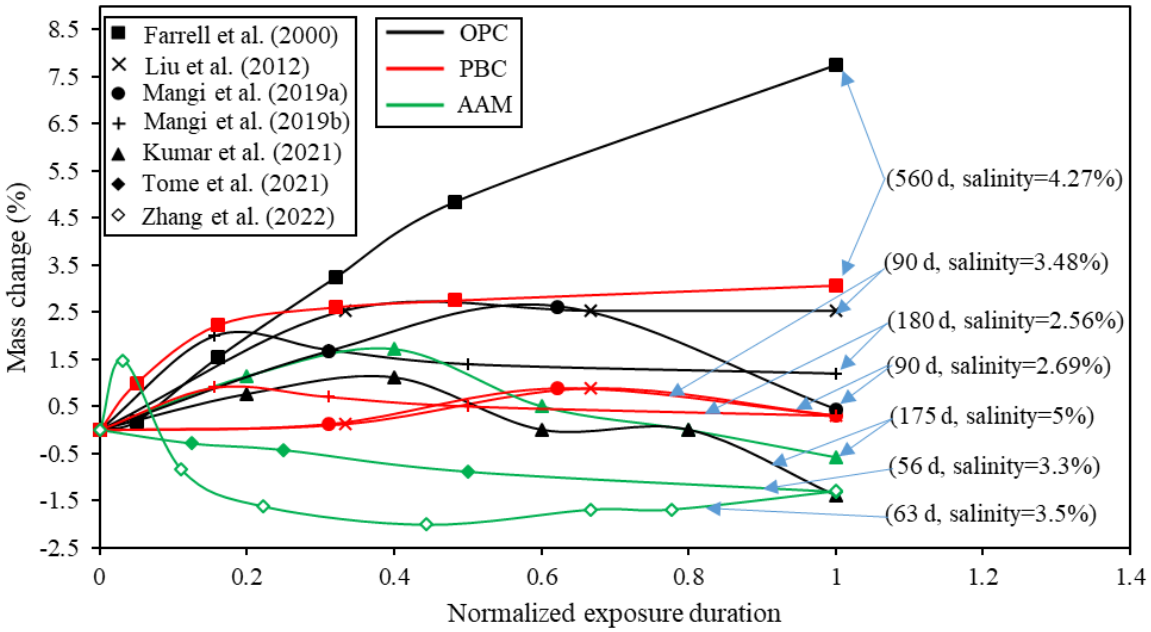

Figure 5. Mass change of cementitious materials exposed to seawater attack (data adapted from [93, 95, 100, 102, 108-110])

Some studies [95, 109, 110] have found distinct patterns of mass change during seawater attack. O'Farrell et al. [95] observed mass increase throughout the exposure period, with the greatest value of 7.8% at 560 days. The study used high strength concrete with 78 MPa grade, which could withstand greater stress caused by formation of more expansive products. Tome et al. [109] showed that lower strength concrete (24 MPa grade) exhibited mass loss throughout test period. The mass loss was due to salt crystallization damage and debris loss of the specimens. Besides, Zhang et al. [110] reported a mass-constant stage following the mass-decreasing stage. The mass-constant stage was due to the exhaustion of reactants in seawater towards the end of the test. Besides, the increase in salinity of seawater also resulted in greater extent of mass variation due to the accelerated seawater reactions.

PBC [93, 95, 100, 102] and AAM [108-110] generally have lower mass variation during seawater attack than OPC. The hydrations of PBC and AAM produce more C-S-H and C-A-S-H, which compacts the pore structure and enhances the seawater resistance. The lack of CH in

PBC and AAM lowers their reactivity with seawater, resulting in fewer products that cause mass change. Pozzolanic materials are often finer than OPC, which provides filling effects to reduce porosity and hence seawater intrusion.

Although mass change has been widely used to evaluate seawater resistance of cementitious materials, its reliability remains controversial because mass change is also caused by water absorption and hydration. It is suggested that other properties such as strength, porosity and permeability should be investigated.

4.3. Porosity and water absorption

Porosity (n) is the ratio of void to total volume of material. Water absorption (WA) is the capability of material to hold water. Both porosity and water absorption can be used to assess the resistance of cementitious materials to seawater penetration. Previous section shows that seawater attack causes mass change due to the development of expansive products and change in hydrate phases, indicating pore structure alteration. As such, the effect of seawater exposure on the porosity and water absorption of OPC, PBC and AAM is determined as shown in Table 2. The porosity and water absorption in seawater environment ($n_{seawater}$, $WA_{seawater}$) are normalized to those in freshwater environment ($n_{freshwater}$, $WA_{freshwater}$).

Table 2. Porosity and water absorption of cementitious materials under seawater attack

Literature	Exposure duration (days)	Cementitious materials	Normalized porosity ($n_{seawater}/n_{freshwater}$)	Normalized water absorption ($WA_{seawater}/WA_{freshwater}$)
Binici et al. [91]	28	OPC	N.D.	0.92
		PBC	N.D.	0.71
Mengasini et al. [98]	56	OPC	0.99	N.D.
		AMM	0.85	N.D.
Puertas et al. [83]	90	AMM	0.83	N.D.
Abdel Rahman and Younes [92]	180	PBC	1.39	N.D.
Ganjian and Pouya [103]	180	OPC	N.D.	0.41
		PBC	N.D.	0.96
Memon et al. [104]	180	OPC	0.9	N.D.
		PBC	0.8	N.D.

Wang et al. [106]	365	PBC	0.88	N.D.

$n_{seawater}$ – porosity in seawater; $n_{freshwater}$ – porosity in freshwater
$WA_{seawater}$ – water absorption in seawater; $WA_{freshwater}$ – water absorption in freshwater
N.D. – Not determined

Table 2 shows that porosity and water absorption are lower in seawater environment than in freshwater environment [83, 91, 98, 103, 104, 106]. Puertas et al. [83] found that the porosity of AAM exposed to seawater was 17% lower than that in freshwater. Memon et al. [104] showed that 180-day seawater attack lowered the concrete porosity by 10%–20%. The water absorption of OPC and SF concrete also reduced by 4%–59% after 180 days of seawater exposure [103]. Seawater ions such as Cl^-, SO_4^{2-}, Na^+ and Ca^{2+} can accelerate the hydration of tri-calcium silicate in cement, promoting formation of hydrate to fill the pore [106]. The precipitation of seawater salts also reduced the porosity. However, Abdel Rahman and Younes [92] found that after 180 days of seawater attack, the porosity of ceramic waste powder paste increased by 39%. The over-accumulation of seawater reaction products could enlarge the pore size and cause cracking.

PBC and AAM generally exhibit greater porosity reduction than OPC. The use of PBC and AAM improves the mechanical resistance, which allows for the accumulation of greater quantities of expansive products. The leaching of CH caused by seawater in PBC and AAM is also lower than in OPC [92]. The hydration of PBC and AAM can reduce the permeability of concrete by nearly 3 times [96]. In short, PBC and AMM are more resistant to seawater attack in terms of porosity and water absorption than OPC.

In comparison to compressive strength and mass change, relatively few studies on porosity and water absorption have been conducted, because they are typically regarded as secondary post-deterioration properties. However, in actual environment, porosity variation during the seawater exposure period is crucial in evaluating the intrusion and deterioration mechanisms, necessitating further research.

4.4. Chloride permeability

The exposure of cementitious materials to seawater leads to chloride penetration. The chloride penetration resistance is determined by chloride permeability and chloride binding capacity. Chloride permeability is governed by porosity and pore size distribution. Chloride binding capacity is attributed to the immobilization of free chloride in terms of Friedel's salt, which has been covered in Section 3. This section therefore assesses the effect of seawater attack on chloride permeability.

Several methods are used to determine chloride permeability, which include rapid chloride permeability test (RCPT), rapid migration test (RMT) and chloride profile test (CPT). Figure 6 depicts the variation of chloride permeability with respect to seawater exposure durations for OPC, PBC and AAM. The chloride permeability generally decreases with exposure duration. Ibrahim et al. [105] showed that when exposure period was increased from 7 to 180 days, the chloride permeability decreased by 40%. Ramachandran et al. [107] demonstrated that the chloride permeability decreased by 28%–63% after 365-day seawater exposure. The reductions in chloride permeability with exposure time were ascribed to the ongoing hydration that densified the pore structure. The precipitation of chloride salts such as calcium chloride and Friedel's salt also reduced the chloride permeability [97]. The formation of ettringite and gypsum products from sulphate reactions suppressed the chloride diffusion [106]. Despite the decreased chloride permeability, Seleem et al. [96] found that after 6-month seawater attack, the maximum chloride content in concrete increased from 0.1% to 0.5%. This chloride content exceeded the 0.15% threshold level, which might trigger corrosion in reinforced concrete.

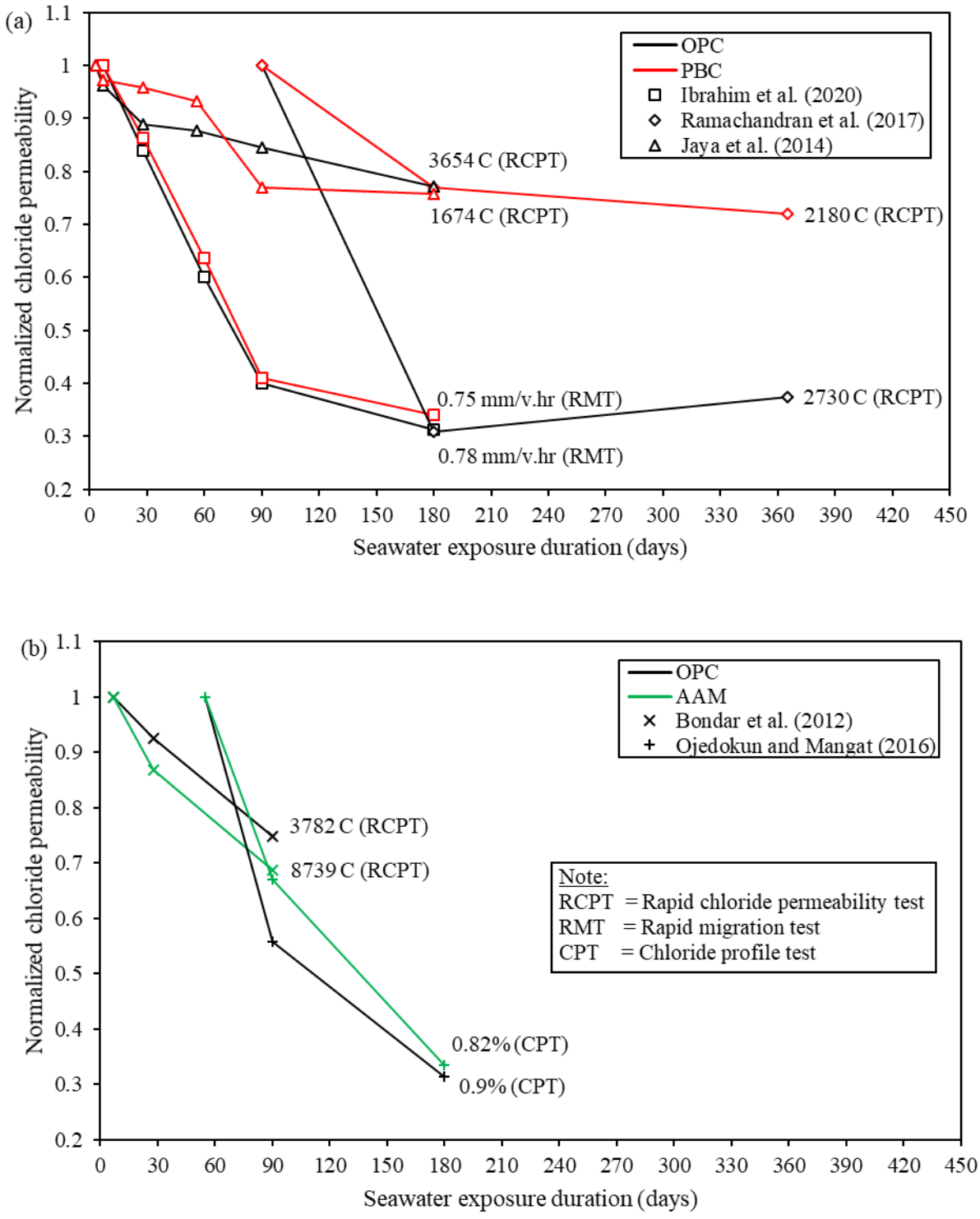

Figure 6. Chloride permeability of OPC, PBC and AAM exposed to seawater environment (data adapted from [97, 105, 107, 111, 112])

Figure 6 also presents the chloride permeability of cementitious materials at the end of each exposure period. Although seawater reduces the chloride permeability of PBC and AAM to

lesser extent, their permeability remains lower than that of OPC. For instance, the use of rice husk ash (RHA) reduced the chloride permeability by half [97]. OPC concrete showed moderate chloride permeability, whereas FA concrete had very low permeability that was equivalent to rock [107]. The 180-day chloride content was reduced from 0.9% to 0.82% after OPC was replaced with AAM [112]. PBC and AAM had greater fineness and binding ability, which bound free chloride and refined pore size distribution. However, Bondar et al. [111] reported that the chloride permeability of AAM was two times that of OPC. This was due to the use of natural pozzolans with lower reactivity in this specific study. But, thermal curing at 40–60^{o}C improved the AAM by decreasing the chloride permeability to level comparable to OPC. In terms of chloride permeability, the use of PBC is better way to reduce seawater attack compared to OPC and AAM.

To summarize, the chloride permeability test is simply an assessment on the permeability of cementitious materials based on chloride intrusion. This property may not accurately reflect the penetration of other seawater components like sulphate and CO_2. Other tests on cementitious materials, such as sorptivity and mercury intrusion porosimetry, are lacking in the existing study and must be investigated further.

4.5. Summary

The external seawater attack influences the hardened-state properties of OPC, PBC and AAM. The literature review has shown contradictory results regarding the effects of seawater on these properties. The hardened-state properties can be deteriorated by seawater through mechanisms such as expansive products formation, salt crystallization and hydrate dissolution. On the other hand, seawater has positive effects on cementitious materials such as pore densification and accelerated hydration. In this context, the assessment on these hardened-state properties could not fully reflect the seawater-induced deterioration mechanism. Seawater attacks the cementitious materials at the surface and propagates into the inner core, causing deterioration

of varying severity along the intrusion path. Hence, future research should investigate this non-uniform and progressive damage caused by seawater. One possible approach is to assess the profile of deterioration products such as chloride, sulphate and CO_2, and then correlate the results with mechanical properties such as stress-strain response.

5. Seawater attack in combination with environmental factors

In practice, seawater attack is often accompanied by environmental factors such as wetting-drying cycle, external service loading and temperature, which can alter the deterioration mechanisms. The laboratory test involving only seawater immersion may not adequately represent actual deterioration. This section looks into the effects of environmental factors.

5.1. Wetting-drying cycle

Seawater exposure in marine environment is divided into four zones, which are atmospheric, submerged, tidal and splash zones [84, 113]. Submerged zone causes constant seawater immersion of structure below sea level. The structure in atmospheric zone is exposed to seawater aerosol. The rise and fall of seawater level in tidal zone and the wave action in splash zone cause periodic exposure of seawater, resulting in wetting-drying cycle (WDC). The WDC promotes moisture transfer and increases ion transport within the porous medium, which aggravates seawater attack.

Figure 7 compares the effects of WDC and full immersion on the strength deterioration of concrete over seawater exposure time. The WDC amplifies the deterioration effects when compared to seawater immersion. Rashad and Sadek [84] showed that the strength degradation in WDC test was 2%–13% higher than that in full immersion test at 365 days. Rashad and Ouda [14] reported that WDC decreased concrete strength by 9.3% more than full immersion after 270-day seawater attack. The WDC exacerbated seawater attack by hastening ettringite and gypsum formations and hydrate dissolution. The damage was also induced by the precipitation

of salt from seawater such as $MgSO_4 \cdot nH_2O$ [99]. Na_2SO_4 salts can precipitate to form thenardite and mirabilite, imposing salt hydration pressure [114]. However, according to some studies [103, 115], both WDC and immersion tests increased strength over time due to pore filling by seawater reaction products. Despite this, a longer exposure period still led to strength reduction. Tang et al. [116] found that although the strength increased due to ettringite formation and accelerated hydration, the WDC caused pore structure loosening and formation of scattered pores larger than 100 nm. The WDC progressively eroded and abraded the surface of cementitious materials. Micro-cracks and cavity developed, and un-bonded particles were found on the cementitious matrix.

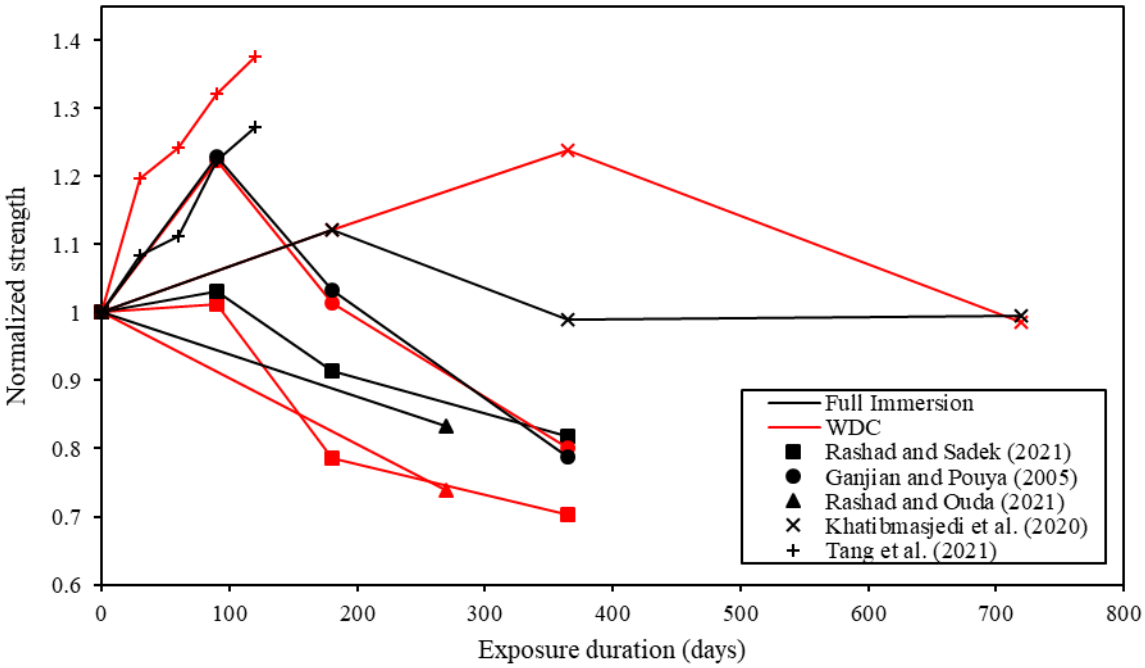

Figure 7. Effect of WDC and full immersion on strength of concrete exposed to seawater attack (data adapted from [14, 84, 103, 115, 116])

The WDC accelerates the seawater intrusion by promoting moisture transfer and ion diffusion. Wu et al. [117] showed that the WDC increased the chloride content by 11.7% to 21.8% when compared to immersion test. Tang et al. [116] demonstrated that the chloride content increased

by 2 times. The WDC accelerated seawater intrusion through the following mechanisms: (1) capillary absorption during the initial wetting phase, (2) continued inward migration during the drying phase as drying occurred from outside to inside, and (3) amplified diffusion due to increased concentration gradient during the subsequent wetting. As the number of WDC grew, more seawater components accumulated at the surface, which enlarged the convection zone. Nonetheless, the use of PBC and AAM might reduce strength deterioration and seawater intrusion by providing nucleation, filler and packing effects on cementitious matrix [14, 84].

5.2. External loading

Structure in service is subjected to loadings such as compression, tension and flexure, which causes stress-strain response that alters pore structure and affects seawater intrusion.

Several studies [118-120] have investigated the influence of compressive loading on chloride penetration. Compressive loading decreases chloride penetration at low stress level while increasing it at high stress level. Bao and Wang [118] found 4% reduction in chloride penetration at stress ratio of 0.3, but 40% increase in penetration at stress ratio of 0.5. Li et al. [119] reported 34.7% drop in diffusivity at stress ratio of 0.6, but 46.1% rise in diffusivity at stress ratio of 0.8. Kim et al. [120] observed 7.7% decrease in permeability at stress ratio of 0.3, but 27.2% increase in permeability at stress ratio 0.6. The reduction in chloride penetration was due to closing of capillary pores under compression that reduced porosity. But, as the load exceeded the critical stress, concrete suffered irreversible damage and cracks formed. The compressive damage increased the width of material interfacial transition zone and chloride penetration.

Tensile and flexural loadings have greater impact on increasing the seawater intrusion. Li et al. [119] showed that the chloride penetration increased with tensile stress level, reaching maximum increase of 67.5% at stress ratio of 0.7. Yoo and Kwon [121] found that tensile

loading resulted in 12.1%–33.9% greater chloride penetration than compressive loading. Cementitious material was intrinsically brittle and had lower tensile resistance than compression. The tensile stress also increased the pore size and caused cracking. Macro-cracks started to develop when tensile stress ratio exceeded 0.3 [120, 122]. The increase in seawater penetration depended on width, length and number of cracks. Seawater can accumulate near crack tips, which amplifies ion diffusion [123]. In addition, external loads in case of cyclic loading resulted in more prominent effects by causing stiffness degradation, fatigue cracking and creeping [124, 125].

5.3. Temperature

In actual environment, structure is exposed to temperature fluctuation due to seasonal and diurnal cycles. During the daytime, the temperature can vary from 30°C to 40°C [126]. The temperature has significant impacts on seawater penetration. Farahani et al. [127] showed that the chloride diffusivity in tidal zone increased by 23.5%–41.6% when temperature increased from 29°C to 34°C. Dousti et al. [128] found that the penetrated chloride concentration increased by twofold as temperature grew from 23°C to 50°C. According to Wang and Ueda [129], the chloride convection zone was expanded by 1.5 times when temperature increased from 23°C to 40°C. Chloride transport was hastened due to the increased diffusion kinetics and faster molecular speed at high temperature. Since the thermal gradient was in the same direction to concentration gradient, the heat flux facilitated the diffusion. The increased temperature also reduced the chloride binding capacity of hydrate phase, decomposing Friedel's salt to release chloride under greater thermal vibration [129]. In addition, the cyclic heating-cooling environment caused drying shrinkage damage [103]. The precipitation of salts, such as $Na_2SO_4 \cdot 10H_2O$, $MgSO_4 \cdot H_2O$ and $MgSO_4 \cdot 6H_2O$, induced salt crystallization pressure [130, 131].

5.4. Summary

Seawater attack is aggravated by environmental factors such as WDC, external loading and temperature. WDC accelerates seawater intrusion and the reactions with cementitious materials. External loading alters pore structure of cementitious matrix, facilitating the penetration of corrosive ions. Elevated temperature induces thermal gradient and increases diffusion kinetics, which promotes seawater ingress. Although the existing studies have reproduced various environmental site conditions in the experiment, their accuracy has not been validated. The outcomes may be imprecise for practical application. Further research is needed to establish correlation between deterioration in laboratory test conditions and actual environments.

6. Discussions and perspectives

In the midst of sea-level-rise crisis, cementitious materials are at risk of premature deterioration due to the intensified seawater attack. Designers and engineers must therefore reassess the durability performance of existing structures; in the worse scenario, reconstruction and rehabilitation are required to ensure compliance with functional requirement standards, which can eventually increase the life-cycle cost. Cementitious materials with more hydrates and less reactants, such as PBC and AAM, offer excellent seawater resistance. They can thus be utilized as protective surface coating on structures to reduce capillary absorption while also acting as barrier against topographical interactions with seawater. Flowability, viscosity and adhesive stability of PBC and AAM can be easily controlled during coating processes like spraying, blading and brushing. The limitation of PBC and AAM is the low pH buffer, which is conducive to seawater-induced hydrate dissolution. Recent technology [132] that uses microcapsule containing hydroxide (OH^-) ions to replenish the CH consumed in seawater reactions, may be adopted.

The external seawater attack influences the hardened-state properties of OPC, PBC and AAM. Due to time constraint, the long-term durability of cementitious materials has not been

adequately researched. Most durability studies have shortened the test durations by adjusting composition, salinity and exposure temperature in order to achieve accelerated seawater reactions. However, the deterioration mechanism of cementitious materials is often inconsistent and can vary based on parameters such as material types, grade, mixture proportions, permeability, as well as curing periods and methods. Furthermore, seawater attack can have both positive effects, such as pore densification and faster hydration, and negative effects, such as expansion, salt crystallization and hydrate dissolution, on the hardened-state properties. The accelerated tests may overestimate the durability requirements, causing the design and selection of cementitious materials that would have performed better and more effectively in the field to be overlooked. Future research can incorporate both long-term field tests and accelerated indoor experiments to validate the test methods and constraints. Computation optimizations [133] such as non-linear statistical regressions and machine learning algorithms can be used to establish their correlations and deliver more credible test result analysis and interpretation.

Seawater attack can be exacerbated when environmental factors such as WDC, external loading and temperature are considered. Table 3 outlines the environmental conditions that have been simulated in the past studies. Researchers adopt various test methods to assess the seawater resistance of cementitious materials based on national standards or customized protocols, which are essentially developed for the study of specific degradation mechanism and laboratory evaluation. The outcomes may be imprecise for practical applications. Further study is needed to establish strong correlation between laboratory tests and actual deterioration by incorporating large-scale field data using methods such as real-time sensor system and automated integration testing [134]. The data can be used to support and develop standard guidelines for assessing the durability of cementitious materials in seawater environment.

Table 3. Environmental conditions considered in laboratory tests of seawater attack

Literature	Wetting-drying cycle	External loading	Temperature	Simulated site
Rashad and Ouda [14]	Wetting: 18 hr Drying: 6 hr	-	-	Tidal zone
Rashad and Sadek [84]	Wetting: 18 hr Drying: 6 hr	-	-	Tidal zone
Farahani et al. [127]	-	-	18–35 ºC	Bandar Abbas, Iran
Wu et al. [117]	Wetting: 8 hr Drying: 8 hr			Bohai Sea; East Sea; Yellow Sea
Hamzah et al. [99]	Wetting: 15 hr Drying: 9 hr	-	-	Malaysia
Jaya et al. [97]	Wetting: 15 hr Drying: 9 hr	-	-	Malaysia
Ting et al. [125]	Wetting: 12 hr Drying: 12 hr	30%–85% cyclic compression	-	Malaysia
Fraternali et al. [89]	Site condition	-	-	Port of Salerno
Ganjian and Pouya [103]	Wetting: 6 hr Drying: 6 hr	-	37–42 ºC	South coast of Iran
Dousti et al. [128]	-	-	22–50 ºC	South coast of Iran
Chen et al. [130]	-	56%–90% cyclic flexure	50 ºC	Subtropical climate
Tang et al. [116]	Wetting: 12 hr Drying: 12 hr	-	60 ºC	Zhairuoshan Island
Liu et al. [124]	Wetting: 10 hr Drying: 38 hr	20%–50% cyclic flexure	80±5 ºC	-
Sahmaran et al. [131]	Wetting: 144 hr Drying: 24 hr	-	100 ºC	-
Bao and Wang [118]	-	10%–50% compression	-	-
Li et al. [119]	-	20%–80% compression 18%–67.5% tension		
Yoo and Kwon [121]	-	30%–60% compression/tension	-	-
Kim et al. [120]	-	30%–60% tension	-	-
Yang and Luo [122]	-	50% flexure	-	-

7. Conclusions

This study reviews the durability of OPC, PBC and AAM exposed to seawater environment in the aspects of chemical interactions and hardened-state properties. The effect of environmental factors including WDC, external loading and temperature on seawater attack has been discussed. Based on the literature review, the following conclusions are drawn:

(1) When exposed to seawater, OPC, PBC and AAM deteriorate due to chemical interactions with chloride, sulphate and CO_2. Seawater reactions consume and deplete the hydrate phases such as C-S-H and CH, resulting in reduced binding capability, increased porosity and loss of alkalinity for corrosion resistance. Although PBC and AAM are more resistant to seawater attack due to the lack of CH and aluminate as reactants, their hydrates like C-A-S-H and N-A-S-H have low Ca/Si ratio, making them susceptible to hydrate decalcification.

(2) After seawater attack, the strength variation is -76% to 51.4% for OPC, -50% to 95.2% for PBC and -42.1% to 62% for AAM. The mass increases at first, but decreases later. The porosity, water absorption and chloride permeability reduces by 1.2% to 15.2%, 0.2% to 28.7% and 22.8% to 68.8% respectively. PBC and AAM minimize the degradation of the hardened-state properties due to the refined pore structure, improved mechanical properties and lower reactivity with seawater.

(3) In general, seawater attack has negative effects on hardened-state properties due to the development of expansive products, salt crystallization and hydrate dissolution. Seawater, on the other hand, has beneficial effects such as pore structure densification and hydration acceleration. Thus, the impact of seawater on durability of cementitious materials is determined by the dominance of positive or negative effects.

(4) Environmental factors of WDC, external loading and temperature exacerbates the seawater attack. WDC hastens moisture transfer and expands water convection zone, accelerating

the transport of corrosive ions. External loading promotes seawater penetration by increasing porosity and causing cracks; though compressive loading below the stress limit can reduce seawater intrusion. The increased temperature speeds up seawater ingress by inducing thermal gradient, which increases the kinetics of ion transport.

Acknowledgement

This research is supported by the Ministry of Education, Singapore, under its Academic Research Fund Tier 2 (MOE-T2EP50220-0004).

Reference

[1] A. Adesina, *Recent advances in the concrete industry to reduce its carbon dioxide emissions.* Environmental Challenges, 2020. **1**: p. 100004.

[2] F. Song, G. J. Zhang, V. Ramanathan and L. R. Leung, *Trends in surface equivalent potential temperature: A more comprehensive metric for global warming and weather extremes.* Proceedings of the National Academy of Sciences, 2022. **119**(6): p. e2117832119.

[3] D. T. Vu, T. Yamada and H. Ishidaira, *Assessing the impact of sea level rise due to climate change on seawater intrusion in Mekong Delta, Vietnam.* Water Science and Technology, 2018. **77**(6): p. 1632-1639.

[4] O. Micheal, B. Glavovic, J. Hinkel, v. Roderik, A. Magnan, A. Abd-Elgawad, C. Rongshu, M. Cifuentes, D. Robert, T. Ghosh, J. Hay, M. Ben, B. Meyssignac, Z. Sebesvari, S. A.J, S. Dangendorf and T. Frederikse, *Sea Level Rise and Implications for Low Lying Islands, Coasts and Communities*. 2019. p. 321-445.

[5] B. Ataie-Ashtiani, A. D. Werner, C. T. Simmons, L. K. Morgan and C. Lu, *How important is the impact of land-surface inundation on seawater intrusion caused by sea-level rise?* Hydrogeology Journal, 2013. **21**(7): p. 1673-1677.

[6] H. Ketabchi, D. Mahmoodzadeh, B. Ataie-Ashtiani and C. T. Simmons, *Sea-level rise impacts on seawater intrusion in coastal aquifers: Review and integration.* Journal of Hydrology, 2016. **535**: p. 235-255.

[7] S. B. Lee, M. Li and F. Zhang, *Impact of sea level rise on tidal range in Chesapeake and Delaware Bays.* Journal of Geophysical Research: Oceans, 2017. **122**(5): p. 3917-3938.

[8] F. Qu, W. Li, W. Dong, V. W. Tam and T. Yu, *Durability deterioration of concrete under marine environment from material to structure: A critical review.* Journal of Building Engineering, 2021. **35**: p. 102074.

[9] D. Jansen, F. Goetz-Neunhoeffer, B. Lothenbach and J. Neubauer, *The early hydration of Ordinary Portland Cement (OPC): An approach comparing measured heat flow with calculated heat flow from QXRD.* Cement and Concrete Research, 2012. **42**(1): p. 134-138.

[10] J. J. Beaudoin, S. Catinaud and J. Marchand, *Volume stability of calcium hydroxide in aggressive solutions.* Cement and Concrete Research, 2001. **31**(1): p. 149-151.

[11] F. U. A. Shaikh and J. Dobson, *Effect of fly ash on compressive strength and chloride binding of seawater-mixed mortars.* Journal of Sustainable Cement-Based Materials, 2019. **8**(5): p. 275-289.

[12] E. Ganjian and H. S. Pouya, *The effect of Persian Gulf tidal zone exposure on durability of mixes containing silica fume and blast furnace slag.* Construction and Building Materials, 2009. **23**(2): p. 644-652.

[13] A. Dasar, D. Patah, H. Hamada, Y. Sagawa and D. Yamamoto, *Applicability of seawater as a mixing and curing agent in 4-year-old concrete.* Construction and Building Materials, 2020. **259**: p. 119692.
[14] A. M. Rashad and A. S. Ouda, *Effect of tidal zone and seawater attack on high-volume fly ash pastes enhanced with metakaolin and quartz powder in the marine environment.* Microporous and Mesoporous Materials, 2021. **324**: p. 111261.
[15] J. L. Provis, *Alkali-activated materials.* Cement and Concrete Research, 2018. **114**: p. 40-48.
[16] J. L. Provis, A. Palomo and C. Shi, *Advances in understanding alkali-activated materials.* Cement and Concrete Research, 2015. **78**: p. 110-125.
[17] F. J. Millero and F. Huang, *The density of seawater as a function of salinity (5 to 70 g kg− 1) and temperature (273.15 to 363.15 K).* Ocean Science, 2009. **5**(2): p. 91-100.
[18] P. Li, W. Li, Z. Sun, L. Shen and D. Sheng, *Development of sustainable concrete incorporating seawater: A critical review on cement hydration, microstructure and mechanical strength.* Cement and Concrete Composites, 2021. **121**: p. 104100.
[19] Y. Yi, D. Zhu, S. Guo, Z. Zhang and C. Shi, *A review on the deterioration and approaches to enhance the durability of concrete in the marine environment.* Cement and Concrete Composites, 2020. **113**: p. 103695.
[20] K. L. Davis, M. A. Coleman, S. D. Connell, B. D. Russell, B. M. Gillanders and B. P. Kelaher, *Ecological performance of construction materials subject to ocean climate change.* Marine environmental research, 2017. **131**: p. 177-182.
[21] S. A. Mangi, A. Makhija, M. S. Raza, S. H. Khahro and A. A. Jhatial, *A comprehensive review on effects of seawater on engineering properties of concrete.* Silicon, 2021. **13**(12): p. 4519-4526.
[22] Y. Zhao, X. Hu, C. Shi, Z. Zhang and D. Zhu, *A review on seawater sea-sand concrete: Mixture proportion, hydration, microstructure and properties.* Construction and Building Materials, 2021. **295**: p. 123602.
[23] J. Xiao, C. Qiang, A. Nanni and K. Zhang, *Use of sea-sand and seawater in concrete construction: Current status and future opportunities.* Construction and Building Materials, 2017. **155**: p. 1101-1111.
[24] E. Samson, J. Marchand, K. A. Snyder and J. J. Beaudoin, *Modeling ion and fluid transport in unsaturated cement systems in isothermal conditions.* Cement and Concrete Research, 2005. **35**(1): p. 141-153.
[25] X. Li, S. Chen, Q. Xu and Y. Xu, *Modeling the three-dimensional unsaturated water transport in concrete at the mesoscale.* Computers & Structures, 2017. **190**: p. 61-74.
[26] S. Poyet, S. Charles, N. Honoré and V. L'Hostis, *Assessment of the unsaturated water transport properties of an old concrete: Determination of the pore-interaction factor.* Cement and Concrete Research, 2011. **41**(10): p. 1015-1023.
[27] O. Truc, J. P. Ollivier and L.-O. Nilsson, *Numerical simulation of multi-species diffusion.* Materials and Structures, 2000. **33**(9): p. 566-573.
[28] E. Samson and J. Marchand, *Modeling the transport of ions in unsaturated cement-based materials.* Computers & Structures, 2007. **85**(23-24): p. 1740-1756.
[29] E. Samson, G. Lemaire, J. Marchand and J. J. Beaudoin, *Modeling chemical activity effects in strong ionic solutions.* Computational Materials Science, 1999. **15**(3): p. 285-294.
[30] S. Alvès, G. Demouchy, A. Bee, D. Talbot, A. Bourdon and A. M. F. Neto, *Investigation of the sign of the Soret coefficient in different ionic and surfacted magnetic colloids using forced Rayleigh scattering and single-beam Z-scan techniques.* Philosophical Magazine, 2003. **83**(17-18): p. 2059-2066.
[31] E. Samson and J. Marchand, *Modeling the effect of temperature on ionic transport in cementitious materials.* Cement and Concrete Research, 2007. **37**(3): p. 455-468.
[32] A. Suryavanshi, J. Scantlebury and S. Lyon, *Mechanism of Friedel's salt formation in cements rich in tri-calcium aluminate.* Cement and concrete research, 1996. **26**(5): p. 717-727.
[33] T. Matschei, B. Lothenbach and F. Glasser, *The AFm phase in Portland cement.* Cement and concrete research, 2007. **37**(2): p. 118-130.
[34] K. De Weerdt, H. Justnes and M. R. Geiker, *Changes in the phase assemblage of concrete exposed to sea water.* Cement and Concrete Composites, 2014. **47**: p. 53-63.

[35] A. Mesbah, M. François, C. Cau-dit-Coumes, F. Frizon, Y. Filinchuk, F. Leroux, J. Ravaux and G. Renaudin, *Crystal structure of Kuzel's salt 3CaO· Al2O3· 1/2CaSO4· 1/2CaCl2· 11H2O determined by synchrotron powder diffraction.* Cement and Concrete Research, 2011. **41**(5): p. 504-509.
[36] P. Li, W. Li, T. Yu, F. Qu and V. W. Tam, *Investigation on early-age hydration, mechanical properties and microstructure of seawater sea sand cement mortar.* Construction and Building Materials, 2020. **249**: p. 118776.
[37] T. U. Mohammed, H. Hamada and T. Yamaji, *Performance of seawater-mixed concrete in the tidal environment.* Cement and concrete research, 2004. **34**(4): p. 593-601.
[38] E. Ariyachandra, S. Peethamparan, S. Patel and A. Orlov, *Chloride diffusion and binding in concrete containing NO2 sequestered recycled concrete aggregates (NRCAs).* Construction and Building Materials, 2021. **291**: p. 123328.
[39] C. Qiao, P. Suraneni, T. N. W. Ying, A. Choudhary and J. Weiss, *Chloride binding of cement pastes with fly ash exposed to CaCl2 solutions at 5 and 23° C.* Cement and Concrete Composites, 2019. **97**: p. 43-53.
[40] P. Suraneni, V. J. Azad, B. O. Isgor and W. J. Weiss, *Calcium oxychloride formation in pastes containing supplementary cementitious materials: Thoughts on the role of cement and supplementary cementitious materials reactivity.* RILEM Technical Letters, 2016. **1**: p. 24-30.
[41] H. E. Álava, N. De Belie and G. De Schutter, *Proposed mechanism for the formation of oxychloride crystals during sodium chloride application as a deicer salt in carbonated concrete.* Construction and Building Materials, 2016. **109**: p. 188-197.
[42] C. Qiao, P. Suraneni and J. Weiss, *Flexural strength reduction of cement pastes exposed to CaCl2 solutions.* Cement and Concrete Composites, 2018. **86**: p. 297-305.
[43] C. Qiao, P. Suraneni, M. Tsui Chang and J. Weiss, *Damage in cement pastes exposed to MgCl2 solutions.* Materials and Structures, 2018. **51**(3): p. 1-15.
[44] M. Nehdi and M. Hayek, *Behavior of blended cement mortars exposed to sulfate solutions cycling in relative humidity.* Cement and Concrete Research, 2005. **35**(4): p. 731-742.
[45] P. J. Tikalsky, D. Roy, B. Scheetz and T. Krize, *Redefining cement characteristics for sulfate-resistant Portland cement.* Cement and Concrete Research, 2002. **32**(8): p. 1239-1246.
[46] U. H. Jakobsen, K. De Weerdt and M. R. Geiker, *Elemental zonation in marine concrete.* Cement and Concrete Research, 2016. **85**: p. 12-27.
[47] K. De Weerdt and H. Justnes, *The effect of sea water on the phase assemblage of hydrated cement paste.* Cement and Concrete Composites, 2015. **55**: p. 215-222.
[48] T. Aye and C. T. Oguchi, *Resistance of plain and blended cement mortars exposed to severe sulfate attacks.* Construction and Building Materials, 2011. **25**(6): p. 2988-2996.
[49] S. Yoon, J. Ha, S. R. Chae, D. A. Kilcoyne, Y. Jun, J. E. Oh and P. J. Monteiro, *Phase changes of monosulfoaluminate in NaCl aqueous solution.* Materials, 2016. **9**(5): p. 401.
[50] O. S. B. Al-Amoudi, M. Maslehuddin and Y. A. Abdul-Al, *Role of chloride ions on expansion and strength reduction in plain and blended cements in sulfate environments.* Construction and Building Materials, 1995. **9**(1): p. 25-33.
[51] Y. Cao, L. Guo, B. Chen and J. Wu, *Thermodynamic modelling and experimental investigation on chloride binding in cement exposed to chloride and chloride-sulfate solution.* Construction and Building Materials, 2020. **246**: p. 118398.
[52] M. Frías, S. Goñi, R. García and R. V. de La Villa, *Seawater effect on durability of ternary cements. Synergy of chloride and sulphate ions.* Composites Part B: Engineering, 2013. **46**: p. 173-178.
[53] K. Samimi, S. Kamali-Bernard and A. A. Maghsoudi, *Durability of self-compacting concrete containing pumice and zeolite against acid attack, carbonation and marine environment.* Construction and building materials, 2018. **165**: p. 247-263.
[54] C.-F. Chang and J.-W. Chen, *The experimental investigation of concrete carbonation depth.* Cement and Concrete Research, 2006. **36**(9): p. 1760-1767.

[55] M. Saillio, V. Baroghel-Bouny and F. Barberon, *Chloride binding in sound and carbonated cementitious materials with various types of binder.* Construction and building Materials, 2014. **68**: p. 82-91.
[56] H. Chang, P. Feng, K. Lyu and J. Liu, *A novel method for assessing CSH chloride adsorption in cement pastes.* Construction and Building Materials, 2019. **225**: p. 324-331.
[57] H. Ye, X. Jin, C. Fu, N. Jin, Y. Xu and T. Huang, *Chloride penetration in concrete exposed to cyclic drying-wetting and carbonation.* Construction and Building Materials, 2016. **112**: p. 457-463.
[58] T. Sibbick, D. Fenn and N. Crammond, *The occurrence of thaumasite as a product of seawater attack.* Cement and Concrete Composites, 2003. **25**(8): p. 1059-1066.
[59] J. Bensted, *Thaumasite—background and nature in deterioration of cements, mortars and concretes.* Cement and Concrete Composites, 1999. **21**(2): p. 117-121.
[60] M. Anwar and D. A. Emarah, *Resistance of concrete containing ternary cementitious blends to chloride attack and carbonation.* Journal of Materials Research and Technology, 2020. **9**(3): p. 3198-3207.
[61] B. Lothenbach, K. Scrivener and R. Hooton, *Supplementary cementitious materials.* Cement and concrete research, 2011. **41**(12): p. 1244-1256.
[62] M. M. A. Elahi, C. R. Shearer, A. N. R. Reza, A. K. Saha, M. N. N. Khan, M. M. Hossain and P. K. Sarker, *Improving the sulfate attack resistance of concrete by using supplementary cementitious materials (SCMs): A review.* Construction and Building Materials, 2021. **281**: p. 122628.
[63] F. Nosouhian, M. Fincan, N. Shanahan, Y. P. Stetsko, K. A. Riding and A. Zayed, *Effects of slag characteristics on sulfate durability of Portland cement-slag blended systems.* Construction and Building Materials, 2019. **229**: p. 116882.
[64] S. Ogawa, T. Nozaki, K. Yamada, H. Hirao and R. Hooton, *Improvement on sulfate resistance of blended cement with high alumina slag.* Cement and Concrete Research, 2012. **42**(2): p. 244-251.
[65] Y. Wang, S. Nanukuttan, Y. Bai and P. Basheer, *Influence of combined carbonation and chloride ingress regimes on rate of ingress and redistribution of chlorides in concretes.* Construction and Building Materials, 2017. **140**: p. 173-183.
[66] M. Saillio, V. Baroghel-Bouny, S. Pradelle, M. Bertin, J. Vincent and J.-B. d. E. de Lacaillerie, *Effect of supplementary cementitious materials on carbonation of cement pastes.* Cement and concrete research, 2021. **142**: p. 106358.
[67] I. Ismail, S. A. Bernal, J. L. Provis, R. San Nicolas, D. G. Brice, A. R. Kilcullen, S. Hamdan and J. S. van Deventer, *Influence of fly ash on the water and chloride permeability of alkali-activated slag mortars and concretes.* Construction and Building Materials, 2013. **48**: p. 1187-1201.
[68] I. Ismail, S. A. Bernal, J. L. Provis, R. San Nicolas, S. Hamdan and J. S. van Deventer, *Modification of phase evolution in alkali-activated blast furnace slag by the incorporation of fly ash.* Cement and Concrete Composites, 2014. **45**: p. 125-135.
[69] O. Kayali, M. Khan and M. S. Ahmed, *The role of hydrotalcite in chloride binding and corrosion protection in concretes with ground granulated blast furnace slag.* Cement and Concrete Composites, 2012. **34**(8): p. 936-945.
[70] M. Khan, O. Kayali and U. Troitzsch, *Chloride binding capacity of hydrotalcite and the competition with carbonates in ground granulated blast furnace slag concrete.* Materials and Structures, 2016. **49**(11): p. 4609-4619.
[71] X. Ke, S. A. Bernal and J. L. Provis, *Uptake of chloride and carbonate by Mg-Al and Ca-Al layered double hydroxides in simulated pore solutions of alkali-activated slag cement.* Cement and Concrete Research, 2017. **100**: p. 1-13.
[72] T. Bakharev, J. G. Sanjayan and Y.-B. Cheng, *Sulfate attack on alkali-activated slag concrete.* Cement and Concrete research, 2002. **32**(2): p. 211-216.
[73] H. Ye, Z. Chen and L. Huang, *Mechanism of sulfate attack on alkali-activated slag: The role of activator composition.* Cement and Concrete Research, 2019. **125**: p. 105868.
[74] M. Komljenović, Z. Baščarević, N. Marjanović and V. Nikolić, *External sulfate attack on alkali-activated slag.* Construction and Building Materials, 2013. **49**: p. 31-39.

[75] I. Ismail, S. A. Bernal, J. L. Provis, S. Hamdan and J. S. van Deventer, *Microstructural changes in alkali activated fly ash/slag geopolymers with sulfate exposure.* Materials and structures, 2013. **46**(3): p. 361-373.
[76] F. Puertas, M. Palacios and T. Vázquez, *Carbonation process of alkali-activated slag mortars.* Journal of materials science, 2006. **41**(10): p. 3071-3082.
[77] T. Bakharev, J. Sanjayan and Y.-B. Cheng, *Resistance of alkali-activated slag concrete to carbonation.* Cement and Concrete Research, 2001. **31**(9): p. 1277-1283.
[78] R. Pouhet and M. Cyr, *Carbonation in the pore solution of metakaolin-based geopolymer.* Cement and Concrete Research, 2016. **88**: p. 227-235.
[79] S. A. Bernal, J. L. Provis, B. Walkley, R. San Nicolas, J. D. Gehman, D. G. Brice, A. R. Kilcullen, P. Duxson and J. S. van Deventer, *Gel nanostructure in alkali-activated binders based on slag and fly ash, and effects of accelerated carbonation.* Cement and Concrete Research, 2013. **53**: p. 127-144.
[80] J. Zhang, C. Shi, Z. Zhang and Z. Ou, *Durability of alkali-activated materials in aggressive environments: A review on recent studies.* Construction and Building Materials, 2017. **152**: p. 598-613.
[81] S. A. Bernal, R. San Nicolas, R. J. Myers, R. M. de Gutiérrez, F. Puertas, J. S. van Deventer and J. L. Provis, *MgO content of slag controls phase evolution and structural changes induced by accelerated carbonation in alkali-activated binders.* Cement and Concrete Research, 2014. **57**: p. 33-43.
[82] H. Yiğiter, H. Yazıcı and S. Aydın, *Effects of cement type, water/cement ratio and cement content on sea water resistance of concrete.* Building and environment, 2007. **42**(4): p. 1770-1776.
[83] F. Puertas, R. Gutierrez, A. Fernández-Jiménez, S. Delvasto and J. Maldonado, *Alkaline cement mortars. Chemical resistance to sulfate and seawater attack.* Materiales de Construccion, 2002. **52**(267): p. 55-71.
[84] A. M. Rashad and D. M. Sadek, *An Exploratory Study on Alkali-Activated Slag Blended with Microsize Metakaolin Particles Under the Effect of Seawater Attack and Tidal Zone.* Arabian Journal for Science and Engineering, 2021: p. 1-12.
[85] A. M. Rashad, A. S. Ouda and D. M. Sadek, *Behavior of alkali-activated metakaolin pastes blended with quartz powder exposed to seawater attack.* Journal of Materials in Civil Engineering, 2018. **30**(8): p. 04018159.
[86] A. Palomo, M. T. Blanco-Varela, M. Granizo, F. Puertas, T. Vazquez and M. Grutzeck, *Chemical stability of cementitious materials based on metakaolin.* Cement and Concrete research, 1999. **29**(7): p. 997-1004.
[87] A. Fernández-Jiménez, I. Garcia-Lodeiro and A. Palomo, *Durability of alkali-activated fly ash cementitious materials.* Journal of Materials Science, 2007. **42**(9): p. 3055-3065.
[88] F. M. Wegian, *Effect of seawater for mixing and curing on structural concrete.* The IES Journal Part A: Civil & Structural Engineering, 2010. **3**(4): p. 235-243.
[89] F. Fraternali, S. Spadea and V. P. Berardi, *Effects of recycled PET fibres on the mechanical properties and seawater curing of Portland cement-based concretes.* Construction and Building Materials, 2014. **61**: p. 293-302.
[90] S. Kumar, *Influence of water quality on the strength of plain and blended cement concretes in marine environments.* Cement and Concrete Research, 2000. **30**(3): p. 345-350.
[91] H. Binici, O. Aksogan, E. B. Görür, H. Kaplan and M. N. Bodur, *Performance of ground blast furnace slag and ground basaltic pumice concrete against seawater attack.* Construction and Building Materials, 2008. **22**(7): p. 1515-1526.
[92] H. A. Abdel Rahman and M. M. Younes, *Performance of irradiated blended cement paste composites containing ceramic waste powder towards sulfates, chlorides, and seawater attack.* Journal of Vinyl and Additive Technology, 2020. **26**(1): p. 24-34.
[93] S. A. Mangi, M. H. W. Ibrahim, N. Jamaluddin, M. F. Arshad and S. Shahidan, *Performances of concrete containing coal bottom ash with different fineness as a supplementary cementitious material exposed to seawater.* Engineering Science and Technology, an International Journal, 2019. **22**(3): p. 929-938.

[94] N. Zhang, H. Li, D. Peng and X. Liu, *Properties evaluation of silica-alumina based concrete: durability and environmental friendly performance.* Construction and Building Materials, 2016. **115**: p. 105-113.
[95] M. O'Farrell, S. Wild and B. Sabir, *Resistance to chemical attack of ground brick–PC mortar: Part II. Synthetic seawater.* Cement and Concrete Research, 2000. **30**(5): p. 757-765.
[96] H. E.-D. H. Seleem, A. M. Rashad and B. A. El-Sabbagh, *Durability and strength evaluation of high-performance concrete in marine structures.* Construction and building Materials, 2010. **24**(6): p. 878-884.
[97] R. P. Jaya, B. H. A. Bakar, M. A. M. Johari, M. H. W. Ibrahim, M. R. Hainin and D. S. Jayanti, *Strength and microstructure analysis of concrete containing rice husk ash under seawater attack by wetting and drying cycles.* Advances in cement research, 2014. **26**(3): p. 145-154.
[98] L. Mengasini, M. Mavroulidou and M. J. Gunn, *Alkali-activated concrete mixes with ground granulated blast furnace slag and paper sludge ash in seawater environments.* Sustainable Chemistry and Pharmacy, 2021. **20**: p. 100380.
[99] A. Hamzah, M. W. Ibrahim and E. Manan. *Carbonation and strength of self-compacting concrete with coal bottom ash exposed to seawater by wetting-drying cycle*. in *IOP Conference Series: Earth and Environmental Science*. 2020. IOP Publishing.
[100] S. A. Mangi, M. H. W. Ibrahim, N. Jamaluddin, M. F. Arshad, S. A. Memon, S. Shahidan and R. P. Jaya. *Coal bottom ash as a sustainable supplementary cementitious material for the concrete exposed to seawater*. in *AIP Conference Proceedings*. 2019. AIP Publishing LLC.
[101] T. Jena and K. Panda, *Compressive strength and carbonation of sea water cured blended concrete.* Int. J. Civil Eng. Technol, 2017. **8**(2): p. 153-162.
[102] R.-j. Liu, Q.-j. Ding, P. Chen and G.-y. Yang, *Durability of concrete made with manganese slag as supplementary cementitious materials.* Journal of Shanghai Jiaotong University (Science), 2012. **17**(3): p. 345-349.
[103] E. Ganjian and H. S. Pouya, *Effect of magnesium and sulfate ions on durability of silica fume blended mixes exposed to the seawater tidal zone.* Cement and concrete research, 2005. **35**(7): p. 1332-1343.
[104] A. Memon, S. Radin, M. Zain and J.-F. Trottier, *Effects of mineral and chemical admixtures on high-strength concrete in seawater.* Cement and Concrete Research, 2002. **32**(3): p. 373-377.
[105] M. W. Ibrahim, A. Hamzah, N. Jamaluddin, S. Mangi and P. Ramadhansyah, *Influence of bottom ash as a sand replacement material on durability of self-compacting concrete exposed to seawater.* Journal of Engineering Science and Technology, 2020. **15**(1): p. 555-571.
[106] W. Wang, S. Xu, Q. Li and S. Dong, *Long-term performance of fiber reinforced cementitious composites with high ductility under seawater attack with different salinities.* Construction and Building Materials, 2022. **317**: p. 126164.
[107] D. Ramachandran, R. George, V. Vishwakarma and U. Kamachi Mudali, *Strength and durability studies of fly ash concrete in sea water environments compared with normal and superplasticizer concrete.* KSCE Journal of Civil Engineering, 2017. **21**(4): p. 1282-1290.
[108] R. Kumar, M. Verma and N. Dev, *Investigation on the Effect of Seawater Condition, Sulphate Attack, Acid Attack, Freeze–Thaw Condition, and Wetting–Drying on the Geopolymer Concrete.* Iranian Journal of Science and Technology, Transactions of Civil Engineering, 2021: p. 1-31.
[109] S. Tome, A. Nana, C. R. Kaze, J. N. Y. Djobo, T. Alomayri, E. Kamseu, M.-A. Etoh, J. Etame and S. Kumar, *Resistance of Alkali-Activated Blended Volcanic Ash-MSWI-FA Mortar in Sulphuric Acid and Artificial Seawater.* Silicon, 2021: p. 1-8.
[110] N. Zhang, A. Hedayat, L. Figueroa, K. X. Steirer, H. Li, H. G. B. Sosa, R. P. H. Bernal, N. Tupa, I. Y. Morales and R. S. C. Loza, *Experimental studies on the durability and leaching properties of alkali-activated tailings subjected to different environmental conditions.* Cement and Concrete Composites, 2022. **130**: p. 104531.
[111] D. Bondar, C. J. Lynsdale, N. B. Milestone and N. Hassani, *Oxygen and chloride permeability of alkali-activated natural pozzolan concrete.* ACI Materials Journal, 2012. **109**(1): p. 53-61.

[112] O. Ojedokun and P. Mangat, *Chloride diffusion in alkali activated concrete*, in *II International Conference on Concrete Sustainability - ICCS16*. 2016, International Center for Numerical Methods in Engineering (CIMNE).
[113] M. Z. Y. Ting, K. S. Wong, M. E. Rahman and S. J. Meheron, *Deterioration of marine concrete exposed to wetting-drying action.* Journal of Cleaner Production, 2021. **278**: p. 123383.
[114] H. Haynes, R. O'Neill, M. Neff and P. K. Mehta, *Salt weathering distress on concrete exposed to sodium sulfate environment.* ACI Materials Journal, 2008. **105**(1): p. 35.
[115] M. Khatibmasjedi, S. Ramanathan, P. Suraneni and A. Nanni, *Compressive strength development of seawater-mixed concrete subject to different curing regimes.* ACI Materials Journal, 2020. **117**(5).
[116] X. Tang, Q. Xu, K. Qian, S. Ruan, S. Lian and S. Zhan, *Effects of cyclic seawater exposure on the mechanical performance and chloride penetration of calcium sulfoaluminate concrete.* Construction and Building Materials, 2021. **303**: p. 124139.
[117] J. Wu, H. Li, Z. Wang and J. Liu, *Transport model of chloride ions in concrete under loads and drying-wetting cycles.* Construction and Building Materials, 2016. **112**: p. 733-738.
[118] J. Bao and L. Wang, *Combined effect of water and sustained compressive loading on chloride penetration into concrete.* Construction & building materials, 2017. **156**: p. 708-718.
[119] H. Li, J. Wu, Y. Song and Z. Wang, *Effect of External Loads on Chloride Diffusion Coefficient of Concrete with Fly Ash and Blast Furnace Slag*. Journal of materials in civil engineering, 2014. **26**(9): p. 4014053.
[120] D. H. Kim, K. Shimura and T. Horiguchi, *Effect of Tensile Loading on Chloride Penetration of Concrete Mixed with Granulated Blast Furnace Slag.* Journal of Advanced Concrete Technology, 2010. **8**(1): p. 27-34.
[121] S.-W. Yoo and S.-J. Kwon, *Effects of cold joint and loading conditions on chloride diffusion in concrete containing GGBFS.* Construction & building materials, 2016. **115**: p. 247-255.
[122] D.-y. Yang and J.-j. Luo, *The damage of concrete under flexural loading and salt solution.* Construction and Building Materials, 2012. **36**: p. 129-134.
[123] Q.-f. Liu, Z. Hu, X.-e. Wang, H. Zhao, K. Qian, L.-j. Li and Z. Meng, *Numerical study on cracking and its effect on chloride transport in concrete subjected to external load.* Construction & building materials, 2022. **325**.
[124] F. Liu, Z. You, A. Diab, Z. Liu, C. Zhang and S. Guo, *External sulfate attack on concrete under combined effects of flexural fatigue loading and drying-wetting cycles.* Construction and Building Materials, 2020. **249**: p. 118224.
[125] M. Z. Y. Ting, K. S. Wong, M. E. Rahman and M. S. Joo, *Cyclic compressive behavior of limestone and silicomanganese slag concrete subjected to sulphate attack and wetting-drying action in marine environment.* Journal of Building Engineering, 2021. **44**: p. 103357.
[126] O. S. B. Al-Amoudi, M. Maslehuddin, M. Shameem and M. Ibrahim, *Shrinkage of plain and silica fume cement concrete under hot weather.* Cement and Concrete Composites, 2007. **29**(9): p. 690-699.
[127] A. Farahani, H. Taghaddos and M. Shekarchi, *Prediction of long-term chloride diffusion in silica fume concrete in a marine environment.* Cement and Concrete Composites, 2015. **59**: p. 10-17.
[128] A. Dousti, R. Rashetnia, B. Ahmadi and M. Shekarchi, *Influence of exposure temperature on chloride diffusion in concretes incorporating silica fume or natural zeolite.* Construction and Building Materials, 2013. **49**: p. 393-399.
[129] L.-c. Wang and T. Ueda, *Meso-scale modeling of chloride diffusion in concrete with consideration of effects of time and temperature.* Water Science and Engineering, 2009. **2**(3): p. 58-70.
[130] Z. Chen, P. Huang, G. Yao, X. Guo, Y. Yang, W. Li and B. Wu, *Experimental study on fatigue performance of RC beams strengthened with CFRP under variable amplitude overload and hot-wet environment.* Composite Structures, 2020. **244**: p. 112308.
[131] M. Sahmaran, T. K. Erdem and I. O. Yaman, *Sulfate resistance of plain and blended cements exposed to wetting–drying and heating–cooling environments.* Construction and Building Materials, 2007. **21**(8): p. 1771-1778.

[132] Y. Wang, G. Fang, W. Ding, N. Han, F. Xing and B. Dong, *Self-immunity microcapsules for corrosion protection of steel bar in reinforced concrete.* Scientific reports, 2015. **5**(1): p. 1-8.
[133] M. A. DeRousseau, J. R. Kasprzyk and W. V. Srubar Iii, *Computational design optimization of concrete mixtures: A review.* Cement and Concrete Research, 2018. **109**: p. 42-53.
[134] Z. Zhu and I. Brilakis, *Comparison of optical sensor-based spatial data collection techniques for civil infrastructure modeling.* Journal of Computing in Civil Engineering, 2009. **23**(3): p. 170-177.